Kaunas University of Technology

Faculty of Mechanical Engineering and Design

Design of Portable Energy Harvesting Device

Master's Final Degree Project

Abdalkader Charbeck
Project author

Assoc. prof. dr. Inga Skiedraite
Supervisor

Kaunas, 2018

Kaunas University of Technology

Faculty of Mechanical Engineering and Design

Design of Portable Energy Harvesting Design

Master's Final Degree Project

Mechatronics (621H73001)

Abdalkader Charbeck
Project author

Assoc. prof. dr. Inga Skiedraite
Supervisor

Assoc. prof. dr. K. Juzėnas
Reviewer

Kaunas, 2018

Kaunas University of Technology

Faculty of Mechanical Engineering and Design

Abdalkader Charbeck

Design of Portable Energy Harvesting Device

Declaration of Academic Integrity

I confirm that the final project of mine, Abdalkader Charbeck, on the topic „Design of Portable Energy Harvesting Device“ is written completely by myself; all the provided data and research results are correct and have been obtained honestly. None of the parts of this thesis have been plagiarised from any printed, Internet-based or otherwise recorded sources. All direct and indirect quotations from external resources are indicated in the list of references. No monetary funds (unless required by law) have been paid to anyone for any contribution to this project.

I fully and completely understand that any discovery of any manifestations/case/facts of dishonesty inevitably results in me incurring a penalty according to the procedure(s) effective at Kaunas University of Technology.

(name and surname filled in by hand)	(signature)

KAUNAS UN IVERSITY OF TECHNOLOGY

FACULTY OF MECHANICAL ENGINEERING AND DESIGN

Study programme MECHATRONIC 621H73001

TASK ASSIGNMENT FOR FINAL DEGREE PROJECT OF MASTER STUDIES

Given to the student: Abdalkader Charbeck

1. Title of the Project:

Design of Portbale Energy Harvesting Device, Nešiojamo energijos kaupimo įtaiso kūrimas

Approved by the Dean Order No. V25-11-6, 12 April 2018

2. Aim and Tasks of the Project:

The aim of this project is to design a portable energy harvesting device, which gives better electric output power through wind flow and human acceleration. The tasks are: to study different piezoelectric materials and substrate materials; to develop cantilever beam which can be used in the portable device; to design several prototype shapes.

3. Initial Data: The wind flow between 1 and 20 m/s, the human motion accelration is 1.2 m/s^2.

4. Main Requirements and Conditions:

Small device, high output velocity of wind flow.

5. Structure of the Text Part:

Introduction, review of energy harvesting methods, prototype design, control unit of energu havresting device, conclusion.

6. Structure of the Graphical Part: Drawings of prototype

7. Consultants of the Project: none

Student Abdalkader Charbeck

Supervisor Assoc. prof. dr. Inga Skiedraite

Programme Director of the Study field Assoc. Prof. Regita Bendikiene

Table of contents

List of figures

List of tables

Abbreviations

AC	Alternating current
CFD	Computational flow dynamic
Cr	Chromium
CPU	Central process unit
DC	Direct current
EH	Energy harvesting
FEA	Finite element analysis
FEM	Finite element method
MEMS	Micro electric mechanical system
PM	Power management
PV	Photo Voltic
PMIC	Power management integrated circuit
PZT	Lead zirconate titanate
PMMA	Poly (methyl 2-methylpropenoate)
SI	Silicon
TE	Thermoelectric energy

Abdalkader Charbeck. Design of Portable Energy Harvesting Device. Master's Final Degree Project/ supervisor Assoc. prof. dr. Inga Skiedraite; Faculty of Mechanical Engineering and Design, Kaunas University of Technology.
Study field and area (study field group): Production and Manufacturing Engineering, Technological Sciences.
Keywords: Energy harvesting, portable device, piezoelectric material (PZT), wind flow.

Kaunas, 2018. 55 pages.

Summary

The purpose of this project is to develop a portable energy harvesting device and analyse its potential from both a theoretical and a simulation standpoint, the latter involving modelling and designing. The project begins with a review of different energy-harvesting methods and several existing applications. Then, a chapter about the effects of piezoelectric materials and their properties is given. This chapter introduces theoretical terms describing piezoelectric materials, simulates several piezoelectric materials, compares substrate materials, and chooses the appropriate material for this study. After that, several prototypes are designed and simulated in computational fluid-dynamics software to evaluate the wind-flow performance and select the prototype that gives high output velocity of wind flow. This is followed by a description of the control unit and storage system used in this thesis and their advantages.

Finally, the complete energy-harvesting device, including the piezoelectric cantilever beam, control unit, and storage system, are introduced. In conclusions are presented received research results.

Abdalkader Charbeck. Nešiojamojo energijos gavybos įrenginio projektavimas. Magistro baigiamasis projektas/ vadovas doc. dr. Inga Skiedraite; Mechaniko inžinerijos ir dizaino fakultetas, Kauno technologijos universitetas.
Studijų sritis ir sritis (studijų srities grupė): Gamybos inžinerija, Technologijos mokslai.
Raktiniai žodžiai: energijos kaupimas, nešiojamasis įrenginys, pjezoelektrinė medžiaga (PZT), vėjo tėkmė.
Kaunas, 2018. 55 puslapiai.

Santrauka

Šio magistro projekto tikslas yra sukurti nešiojamąjį energijos taupymo įrenginį ir išnagrinėti jo potencialą tiek teoriniu, tiek modeliavimo būdu, kuris ir įrenginio projektavimą. Pradžioje apžvelgiami skirtingi energijos kaupimo metodai ir jau esamus įrenginius. Sekančiame skyriuje pateikiama analizė apie pjezoelektrinių medžiagų pasirinkimą ir jų savybių poveikį. Taip pat šiame skyriuje pateikiami kelių pjezoelektrinių medžiagų tyrimas, palyginus juos ir pasirenkama tinkamiausia medžiaga šiam tyrimui. Toliau naudojant skaičiavimo skysčių-dinamikos programą, yra suprojektuojami ir tyrinėjami keli prototipai, kad įvertinti vėjo srauto našumą. Pasirenkamas prototipas, kuris užtikrina didžiausią vėjo srauto greitį. Valdymo dalyje pateikiamas šiame darbe naudojamas valdymo blokas bei energijos kaupimo sistema ir jų privalumai.

Gale pristatomas energijos kaupimo įrenginio dizainas, kuriame yra pjezoelektrinė gembinė siją, valdymo blokas ir energijos kaupimo sistemą. Išvadose pateikiami gauti rezultatai.

Introduction

Energy harvesting (EH) is the method of extracting energy from external sources and storing it. It makes it possible for sensors and small devices to be self-supplied instead of requiring battery changes.

The demand for sensors is increasing rapidly. All these sensors require batteries for power supply, which entails battery replacement and more expenses. The alternative solution to this problem is EH, i.e. converting the surrounding energy to electrical power for sensors.

The most popular energy harvesting methods are presented in this thesis. Additionally, power management and storage systems are explained.

There are different methods for energy harvesting such as the use of piezoelectric materials, photovoltaic cells, thermoelectric generator, and electromagnetism.

An EH system consists of ambient energy (energy source) such as vibration, thermal energy, or solar energy, a harvester like a piezoelectric material or solar cell, power management, and storage system. (Figure 1).

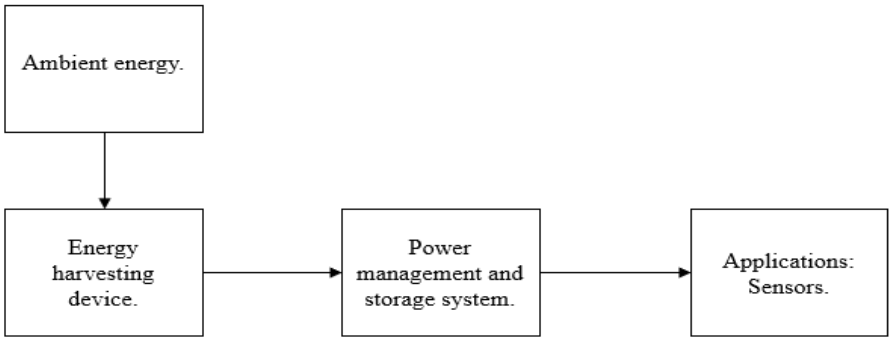

Figure 1. EH system

Aim

The aim of this thesis is to design a portable energy harvesting device that can be used by walkers, which gives better electric output power through wind flow and human acceleration.

Tasks

1. Analyse different Energy harvesting methods and devices.

2. Develop power management and control units.

3. Study and evaluate different piezoelectric materials and substrate materials to select the appropriate materials that can be used to develop a piezoelectric transducer.

4. Propose several shapes by studying the performance of the wind flow through each one of them and choose the shape that gives the highest output velocity

1. Review of energy harvesting methods

1.1. Photovoltaic (PV) cells energy harvesting

A solar cell converts light energy into electricity. It produces higher electric power compared to other EH methods [1]. Figure 2 shows a example of the solar cell system.

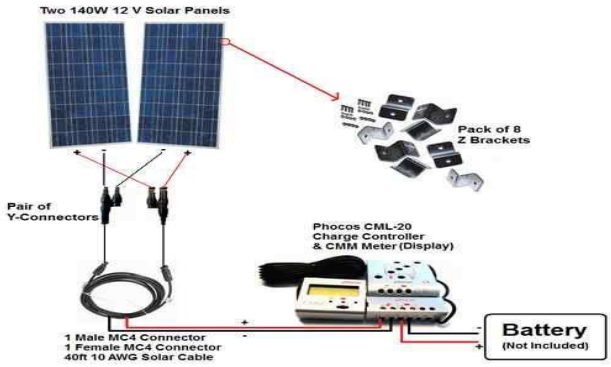

Figure 2. Solar cells (2)

Electric energy produced by photovoltaic cells is clean because it depends on light. At the same time, solar cell is a variable energy source because of its dependence on light.

1.2. Thermoelectric (TE) energy harvesting

Thermoelectric energy harvesters directly convert heat into electricity. A thermoelectric harvester consists of two joined materials P-type and N-type semiconductors. Due to the temperature differences between the two materials, a direct electric current flows in the circuit [3].
The model construction of the TE generator is presented in Figure 3.

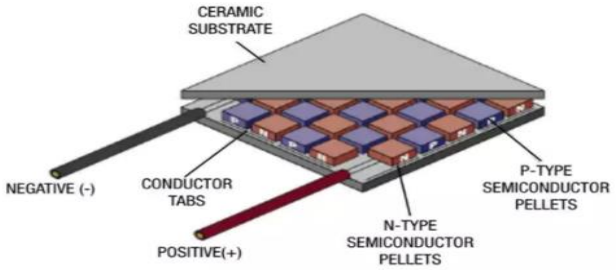

Figure 3. Thermoelectric generator module construction [4]

The output voltage is generally low compared to other EH methods.

1.3. Piezoelectric energy harvesting

Various structures and materials for bulk -type piezoelectric EH are investigated. Many enhancements are added to get the best and most efficient design for a lot of applications. The performance of the

energy harvester is highly affected by acceleration, vibration, applied force, mass, and the surrounding environment.

Piezoelectric effect

The principle of the piezoelectric effect is based on converting mechanical strain into electric voltage. There are a lot of vibration sources such as human motion and wind flow [5].
The piezoelectric cantilever beam configuration is described in Figure 4.

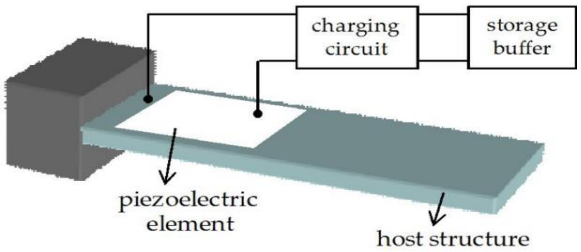

Figure 4**.** Configuration of piezoelectric energy harvester [6]

Cantilever-type piezoelectric energy harvesting

A cantilever electricity harvester is among the promising structures to get high output power from the electrical component. A general structure of the cantilever energy harvester is illustrated in Figure 5 The harvester consists of the piezo-ceramic, elastic body, and proof mass. This straightforward structure produces deformation under vibration and effectively collects the voltage from the electricity ceramic. Every physical aspect of the devices (length, area, mass, thickness, position of the electricity ceramics and elastic body, etc.) determines the operational performance of the harvester.

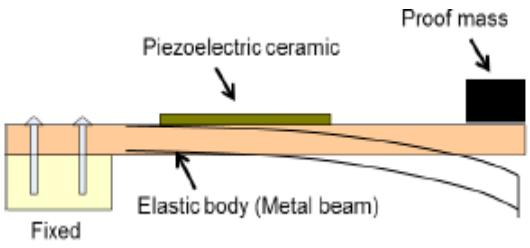

Figure 5. Schematic of cantilever-type piezoelectric energy harvester [7]

Many researchers [7] have investigated the simple cantilever. Additionally, different piezoelectric materials have been used. The low- and high-resonant frequency of the beam determines the application field in the vibration conditions. The comparison of output performance of the bulk cantilever energy harvesters is shown in Table 1.

Table 1. Comparison of the output performance of the cantilever-type bulk piezoelectric harvester [7]

Structure	Power Density (mW/cm3)	Normalized power (mW/g2)	Frequency (Hz)
Cr- and Nb-doped PZT cantilever	2.1	1.1	20
PZNN cantilever	231	11.7	84
<110> oriented single crystalline PMN-PT cantilever	-	3.8	84
<001> oriented single crystalline PMN-PT cantilever	-	1.4	86
PMN-PZT single crystalline cantilever	-	0.2	819
Meandering-structured cantilever	0.2	2.9	50
S-shaped bulk cantilever	8.5	-	40
Wideband LTCC cantilever arrays	-	0.03	1100-1165

Galloping piezoelectric energy harvester

This device harvests energy from ambient structural vibrations using piezoelectric materials. It has been investigated by Sirohi et al. [8].

It is designed as the galloping of a bar with a triangular cross-section hooked up to a cantilever beam (Figure 6). The piezoelectric sheets mounted on the beam convert the mechanical stress into electricity. The device dimensions are 160 mm × 250 mm. The highest output power is 53 mW at a wind speed of 5.20 m/s.

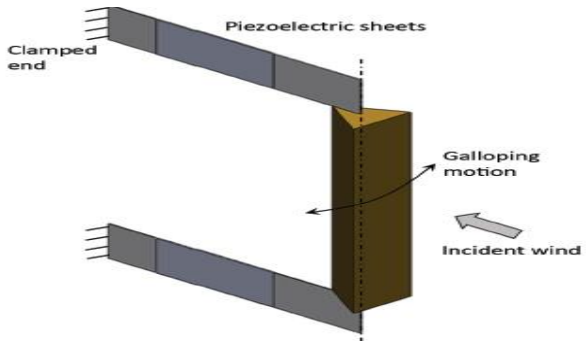

Figure 6. Galloping energy harvester with tip body having an equilateral-triangle cross-section [8]

Flexible piezoelectric sheet

This harvester consists of piezoelectric and flexible materials and has been presented by Mutsuda et al. [9]. This device responds to low wind velocity. The structure has three layers; two layers are made of piezoelectric materials and the third one is a substrate (thin rubber, thin silicone, or fibre) located between the other two layers. This layer has to be light and thin to reduce the weight and increase the deformations. Figure 7 shows a piezoelectric sheet. The average electric power is 82 mW at 12 m/s.

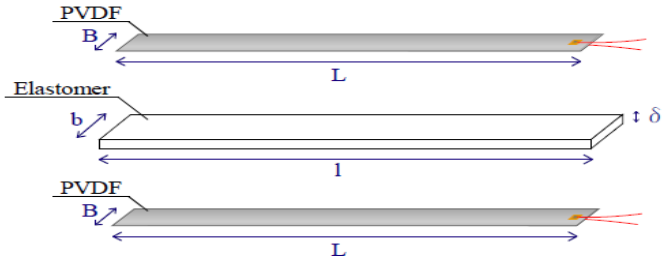

Figure 7. Flexible Piezoelectric Sheet [9]

The piezoelectric material inside the Helmholtz resonator

The main task of the resonator is to convert airflow energy to air oscillations. After that, the oscillations is converted into electrical power by the piezoelectric material.

Figure 8. Helmholtz resonator with the piezoelectric material [10]

The design (Figure 8) of this device depends on a piezoelectric cantilever beam packaged in vacuum between two glass covers. The piezoelectric cantilever beam is mounted at the top of the membrane to maximize the output.

According to a study done by Matova et al. [10], the maximum electrical output is 42.2 μW at 20 m/s.

Flapping cantilevered piezoelectric beam

The wind generator used in this study relies on the oscillation of the cantilever mounted in the direction of the airflow. According to Figure 9, an aerofoil is attached to the end of the free cantilever spring, while the other side is clamped. Air flow in the direction of the aerofoil goes up and down; this produces deflection in the piezoelectric material, the result of which is electrical power.

The power ranges from 0.1 to 0.86 μW at 1.5 m/s to 8 m/s. This device was designed by H Sun et al. [11].

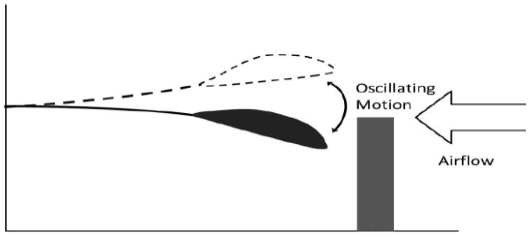

Figure 9. The operation principle of the flapping generator [11]

1.4. Electromagnetic energy harvesting

The main idea behind electromagnetic induction is generating electricity from the relative motion between a conductor and a magnetic field [12].(Figure 10).

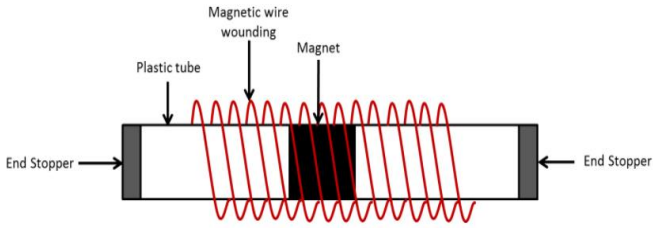

Figure 10. Electromagnetic vibrations energy harvester [13]

The high mass of this device and the low output voltage are the main drawbacks of using the electromagnetic induction method in an EH device.

Electromagnetic energy harvesting device

The basic principle of electromagnetic technology relies on Faraday's law of magnetic force induction. It has been discovered that once the electrical conductor passes through a flux, a possible distinction is evoked between the ends of the conductor.

The number of coil turns and resistance are important parameters for determining the voltage and power produced by a generator.

Soon-Duck Kwon et al. [14] presented an electromagnetic generator with repulsively stacked magnets for harvesting energy from traffic-induced bridge vibrations. Figure 11(a) shows the configuration of a vibration-based energy harvester consisting of a permanent magnet and a solenoid coil. The structure of the multi-layered device is shown in Figure 11 (b). The poles of the magnet units are organized to supply repulsive forces to one another. The poles increase the radial component of magnetic density, which induces a current in the coil; after this, power is generated.

The average power generated from the vibrations of a bridge is 0.98 mW.

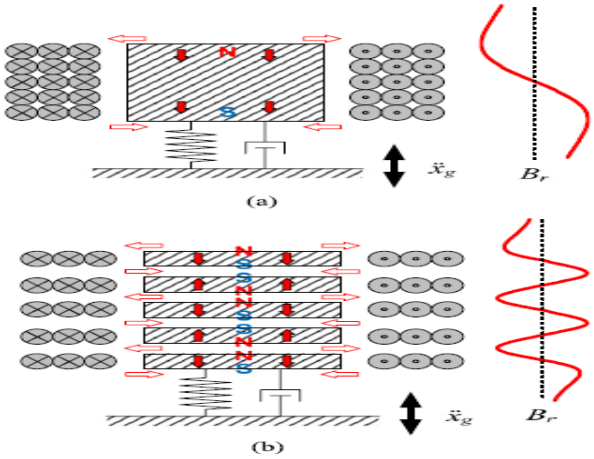

Figure 11. Magnet structures and radial magnetic flux density of electromagnetic energy harvester. (a) Conventional single magnet and coil. (b) Repulsively stacked multi-layered magnets and independent coils [14]

Helmholtz resonator-based technique for energy harvesting

This technique was introduced by Kim et al. [15]. The Hermann von Helmholtz resonator-based energy harvester is shown in Figure 12.

The Hermann von Helmholtz resonator comprises a chamber full of gas (air), with an open neck near the middle. The air in the chamber shows spring behaviour and the air in the neck acts as a diaphragm (membrane). The wall of the resonator is connected with a magnet fixed to this diaphragm. When fluidic oscillation happens in the diaphragm owing to the mechanical energy of wind flow, the magnet connected to the diaphragm vibrates vertically within the coil.

This device includes two components—a cylindrical chamber with 9mm diameter and 5mm height and a neck near the middle of the chamber with 3mm diameter and 5mm height. Peak-to-peak voltage output could be 4 mV at 5 m/s wind speed. However, the facility conversion potency of the proposed wind-energy harvester is quite low even at high wind speed. [15].

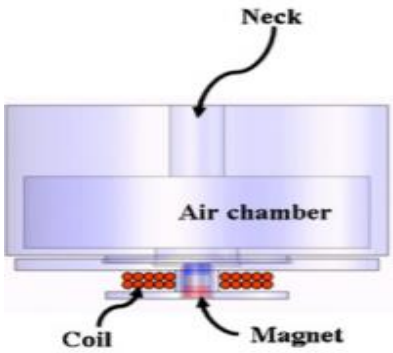

Figure 12. Schematic diagram of the Helmholtz resonator-based energy scavenger [15]

1.5. Advantages and disadvantages of different energy harvesting methods

There are several methods to harvest energy. Table 2 compares the advantages and disadvantages of several EH methods.

Table 2. The advantages and disadvantages of different EH methods

Material	Advantages	Disadvantages
Piezo materials	High output voltage Can be manufactured in small scale Easy coupling	High output impedance Fragile
Electromagnetic	Easy modelling Cheap material	Not very scalable Low output voltage High mass
Magnetostrictive	Easy coupling High flexibility	Hard to model Nonlinear behaviour
Photovoltaic	High output voltage	Light dependency

Finally, the selection of EH method for generating electric power depends on the application.
Due to the specification of this research and energy sources, some of the EH methods are excluded. The EH method used in this research uses piezoelectric materials because the energy sources are wind flow and human acceleration.

The advantages of using piezoelectric materials are the high electric output voltage and small-scale manufacturability to fit the dimensions of the EH device.

2. Selection of piezoelectric materials

The different properties of piezoelectric materials that are considered for the proposed EH device in this section. Additionally, several piezoelectric materials are studied to construct the optimized piezoelectric cantilever beam.

2.1. Piezoelectric material properties and types

This type of material is considered as smart. When force is applied on the surface of a piezoelectric material, the material generates stress, which creates surface deformations. The result of deformations is an electrical voltage across the material. This is known as the piezoelectric effect.
In contrast, the reverse effect is to apply an electric voltage to the piezoelectric material to produce mechanical deformations.
For these reasons, piezo materials can be used for both sensing and actuating elements.

Hooke's law describes the mechanical behaviour of piezoelectric materials [16]:

$$S = sT \tag{1}$$

Where S- strain; s-the inverse of the Young's modulus; T- the external stress.

The stress elongates the material. The elongation of the material is divided by the length to get the strain. The previous equation shows how the strain increases on increasing the external stress.

The electrical behaviour is described by [16]:

$$D = \varepsilon_r \varepsilon_0 E \tag{2}$$

Where D- the electric charge displacement; ε_r- the relative permittivity; ε_0- the minimum value of permittivity $\varepsilon_0 = 8.85\ x\ 10^{-12}\ \frac{F}{M}$; E-the electric field strength.

The electric field strength E and the electric charge displacement are linearly related through the electric permittivity ε.

The ability of EH of different piezo materials depends on the piezoelectric coupling coefficient K. The coupling coefficient describes the coupling between two surfaces according to the following formula:

$$K_{ij} = \frac{d_p}{\sqrt{s\varepsilon}} \tag{3}$$

The piezoelectric coupling coefficient plays an important role in measuring the efficiency of piezoelectric materials in transferring energy from mechanical to electrical domains. $K_{33} and\ K_{31}$ are out of plane and in plane respectively. Table 3 presents the coupling coefficients of several piezoelectric materials.

Table 3. Coupling coefficients of several piezoelectric materials [17]

Material	K_{33}	K_{31}
PZT-4	0.35	0.22
PZT-5A	0.53	0.40
PZT-5H	0.70	0.41
PZT-5J	0.85	0.47
PZT-2	0.43	0.33
PZT-4D	0.41	0.38
PZT-7A	0.30	0.21
PZT-8	0.33	0.23

The coupling coefficients of different materials are studied to identify the appropriate piezo material that can be used to develop the piezoelectric cantilever beam of the EH device.

PZT-5J has high coupling coefficient and can be considered as an appropriate material for this research.

Although PZT is brittle, it is appropriate for EH application due to its high coupling coefficient.

2.2. Configuration and poling direction of the piezo material

PZT material has two different types of configuration. The first type is a single layer of piezoelectric material. The second type is bimorph; it consists of two layers of piezoelectric material [16].

Figure 13 shows a cantilever beam with the axis NA. In the normal state of the cantilever beam, the beam has zero stress and strain at the NA. If the beam bends upwards, it will be in compression above the NA and in tension below the NA.

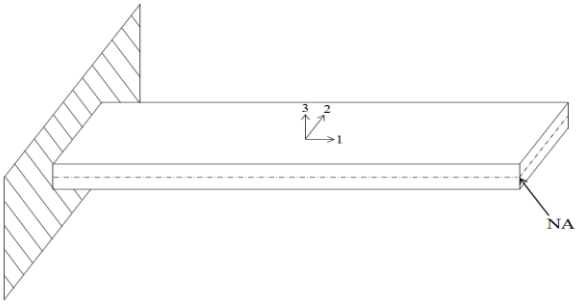

Figure 13. Cantilever beam with the axis [16]

If the piezoelectric material has the first configuration, i.e. single layer, the top of the beam will produce a voltage and the bottom will produce the same voltage but with the opposite sign. In this case, these two voltages will cancel each other out, making the net output voltage zero.

If the piezoelectric material has the second configuration, i.e. two piezoelectric material layers, the layers would have the same dimension and geometry and the NA axis would be between them. If the beam bends upwards, the top layer would be in compression and the bottom layer would be in tension. This would result in two different voltages from two different voltage sources.

The second configuration, i.e. bimorph, is the best for this research, since a single layer will give zero voltage.

The bimorph beam acts as two separate voltage sources, as mentioned before. The sign of each source is regulated by the poling direction of the layers.

A parallel connection of two layers are poled in the same direction. In Figure 14, the direction of the poling is indicated by an arrow. During vibration, one of these layers is in compression and the other is in tension. So, the output voltages from the two layers have different signs.

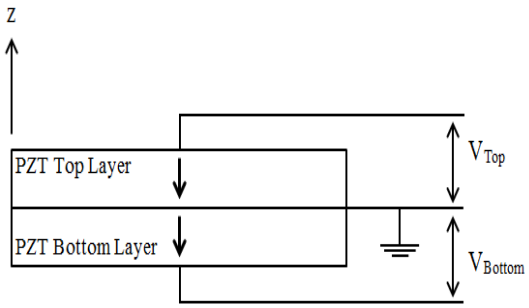

Figure 14. Parallel connection of two PZT layers [16]

Figure 15 shows the equivalent circuit of the parallel connection of two PZT layers.

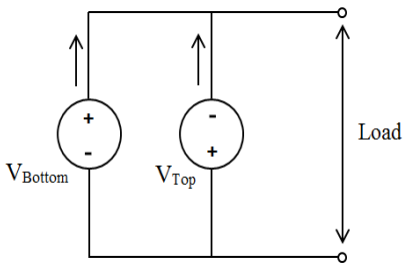

Figure 15. Equivalent circuit of the parallel connection of two PZT layers [16]

In contrast, when the two layers are poled in the opposite direction, as shown in Figure 16, one layer will be in compression and the other in tension. So, the produced voltages would have the same sign. The equivalent circuit of the two voltage sources is a series.

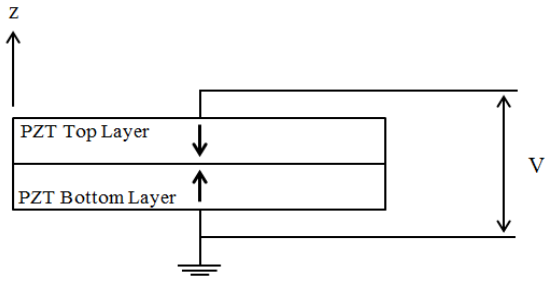

Figure 16. Series connection of two PZT layers [16]

The equivalent circuit is a series connection, as shown in Figure 17

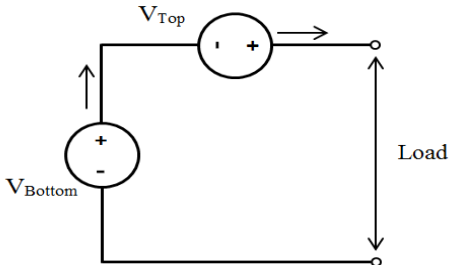

Figure 17. Equivalent circuit of the series connection of two PZT layers [16]

The series configuration is much better than the parallel configuration because the resulting voltage from series is much higher than that from parallel. In EH applications, it is favourable to have a higher voltage to allow for some potential loss. Based on this, the piezoelectric transducer used in this research is designed to be in a series configuration.

2.3. Mechanical modelling of piezo material energy harvesting

The piezoelectric transducer model is explained here. The system consists of a vibrating piezoelectric structure and a PM system.

The vibrating piezoelectric transducer has a mass, spring, and piezo structure, as shown in Figure 18.

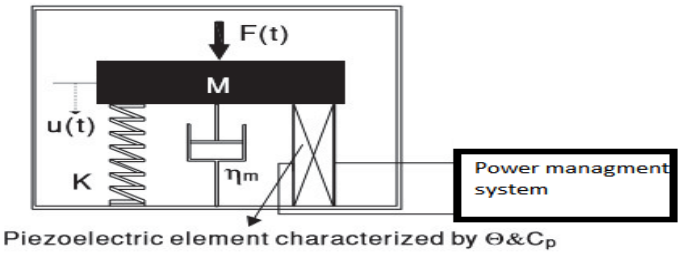

Figure 18. Mechanical model of piezoelectric generator [18]

The piezoelectric element is coupled to a mechanical structure, which is modelled as the second order mass *M*, a spring coefficient *K*, and damping coefficient μ_m.

The effective piezoelectric element θ and capacitance C_p are the main two components of the piezo element. They are related to the geometry and material of piezoelectric material as well as the load direction.

An excitation force is applied to the system. The displacement of the mass is described by u and the voltage in the piezoelectric element is *Vp*. The equations of a vibrating structure are divided into mechanical and piezoelectric elements, as described by [18]:

$$M\ddot{u}(t) + \mu_m\dot{u}(t) + ku(t) + \theta V_p(t) = F(t) \quad (4)$$

$$-\theta\dot{u}(t) + C_p\dot{V}_p(t) = -I(t) \quad (5)$$

$F(t)$- Excitation function; *U*- displacement of the mass; V_p- voltage across the piezo element; $I(t)$- current into the circuit

The previous equations describe the mechanical and electrical modelling of the piezoelectric generator of the piezoelectric transducer of an EH device.

2.4. Piezoelectric material of cantilever beam

Different piezoelectric materials are studied to select the piezoelectric material with low eigenfrequency and better electric output.

COMSOL Multiphysics is used for the finite element analysis of the cantilever beam. The study uses a convenient sample of eight piezoelectric materials, which are compared in terms of eigenfrequency and coupling coefficient.

Figure 19. Beam layers

Each of these eight piezoelectric materials is modelled as a cantilever beam to analyse the eigenfrequency. Then, the piezoelectric material with low eigenfrequency and better electric output is selected for developing the piezoelectric cantilever beam. The cantilever beam is fixed at one side

while the other side is free. It consists of three layers two piezoelectric material layers (40 mm × 20 mm × 0.1 mm) and one substrate material between them (40 mm × 20 mm × 0.1 mm), as shown in Figure 19.

The length and thickness of the cantilever beam are optimized to have eigenfrequency as low as possible to respond to the low wind speed and human motion and maximize the output electric power.

Table 4 shows the design parameters of the cantilever beam, which are used in COMSOL Multiphysics to calculate the electric output power.

Table 4. Design parameters of cantilever piezoelectric beam

Design parameters	**Description**	**Values**
Beam geometry	Structure steel [$L \times W \times$ H]	$40 \times 10 \times 0.1 mm^3$
PZT layer geometry	2 × PZT 5-J [$L \times W \times$ H]	$40 \times 10 \times 0.1 mm^3$
Mass geometry	Material: Tungsten [$L \times W \times H$]	$10 \times 10 \times 3\ mm^3$
Proof mass	The weight of proof tungsten mass	5.7 g
R_load	Load resistance	70 kohm

The cantilever piezoelectric beam with proof mass is constructed to be an optimized oscillator. The material of proof mass is tungsten, which is chosen because it is smaller in size and denser in weight.

Different substrate materials both metal (structure steel) and non-metal (SI, PMMA) are investigated to develop a cantilever beam with low eigenfrequency and high output power. Table 5 provides the properties of different substrate materials.

Table 5. Material properties of different substrate materials

Material	**PMMA**	**SI**	**Structure steel**
Tensile strength	48–76 MPa	113 MPa	130 MPa
Shear modulus	3–3.5 GPa	60 GPa	82 GPa
Poisson's ratio	0.35–0.4	0.28	0.30
Density	1170 kg/m3	2328 kg/m3	7850 kg/m3

The results, as shown in Figure 20, indicate that PZT-5J material has lower eigenfrequency compared to the other piezoelectric materials. Based on this, PZT-5J is an appropriate material for this research. Additionally, although the substrate material has an influence on the eigenfrequency of the cantilever beam, the selection of substrate material is based not only on the low eigenfrequency but also on the electric output power.

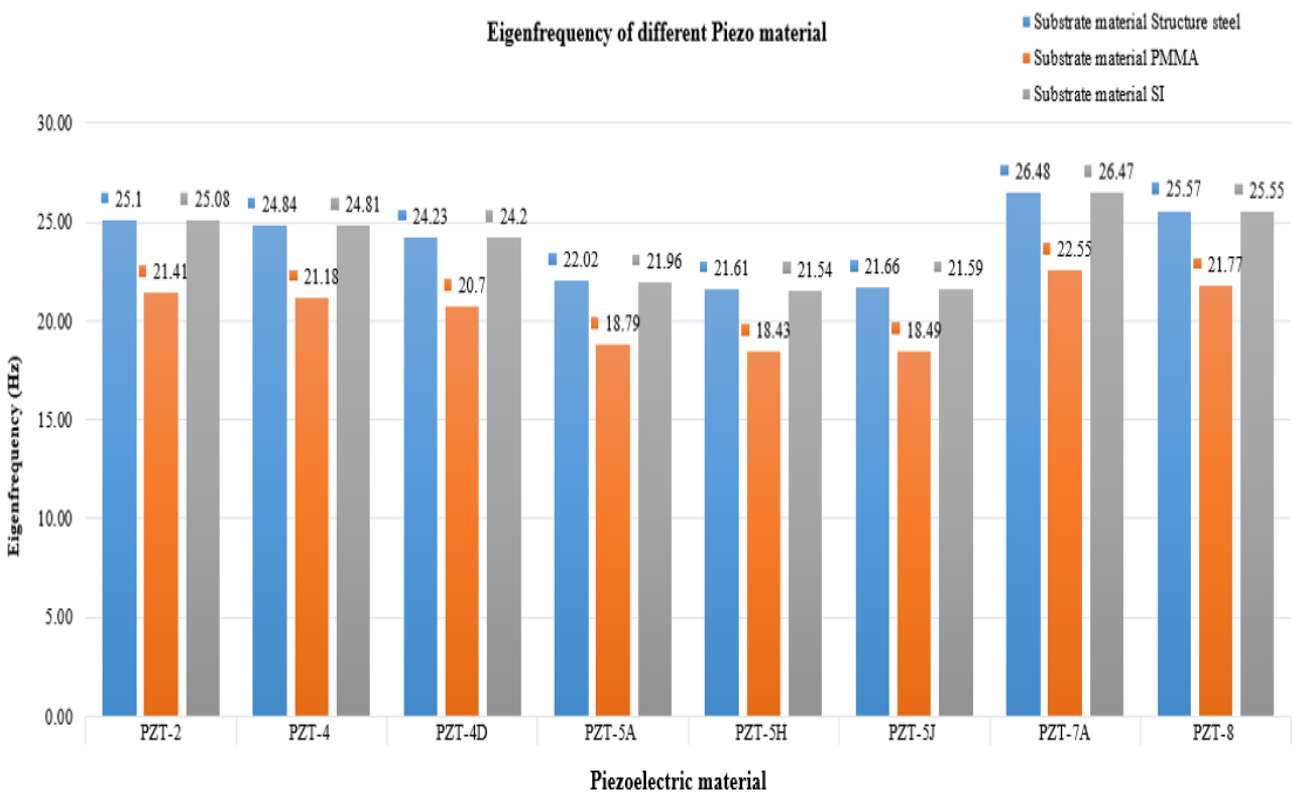

Figure 20. Eigenfrequency of several piezoelectric materials and substrate materials

The results obtained from the eigenfrequency analysis of several piezoelectric and substrate materials are set out in Table 6.

Table 6. Eigenfrequency of several piezoelectric materials and substrate materials

Piezoelectric/ Substrate material	**PZT-2**	**PZT-4**	**PZT-4D**	**PZT-5A**	**PZT-5H**	**PZT-5J**	**PZT-7A**	**PZT-8**
Structure steel	25.1 Hz	24.84 Hz	24.23 Hz	22.02 Hz	21.61 Hz	21.66 Hz	26.48 Hz	25.57 Hz
PMMA	21.41 Hz	21.18 Hz	20.70 Hz	18.79 Hz	18.43 Hz	18.49 Hz	22.55 Hz	21.77 Hz
SI	22.08 Hz	24.82 Hz	24.20 Hz	21.96 Hz	21.54 Hz	21.59 Hz	26.47 Hz	25.55 Hz

Table 6 shows the eigenfrequency of several piezoelectric materials with different substrate materials, the best piezoelectric material is PZT-5j. The substrate material has been chosen according to the electric output.

To compare the electric output voltage, a specific amount of force is applied on the PZT-5J cantilever beam with different substrate materials. As per the proposed boundary conditions, the applied force is 1 [N] and the load resistance is 70 [kΩ]. Results are shown in the following figure 21.

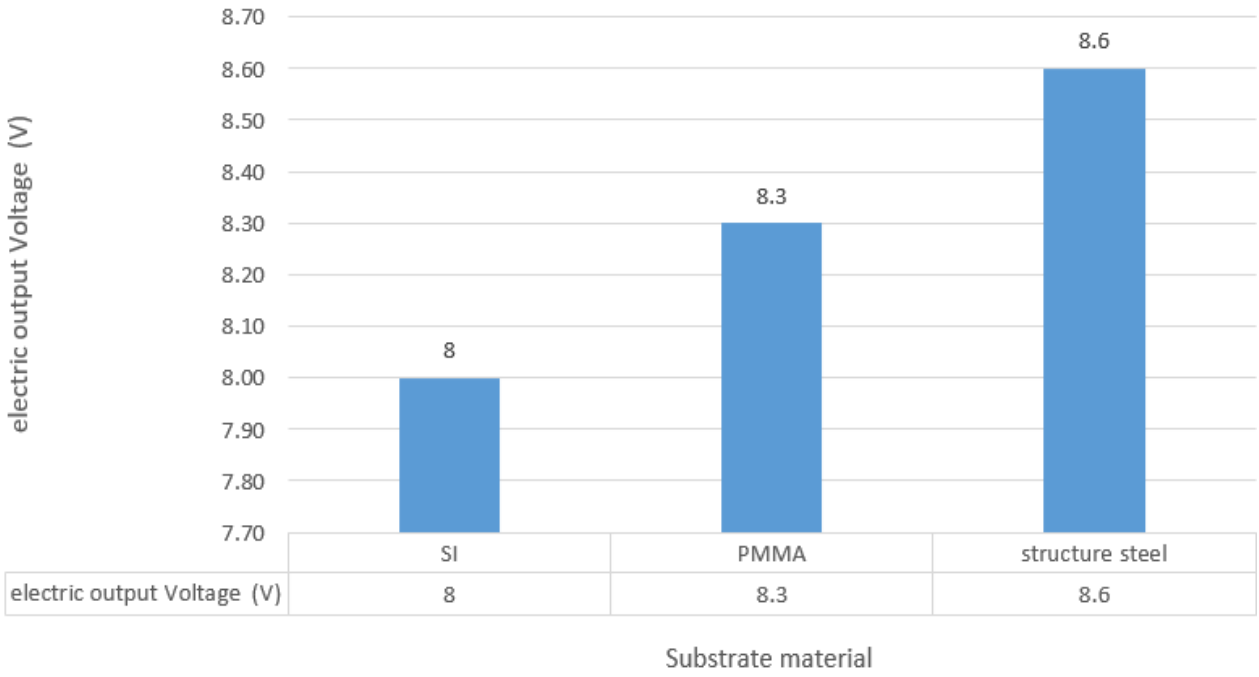

Figure 21. Electric output voltage from PZT-5J with different substrate materials

As shown in Figure 21 the cantilever beam with structure steel substrate material generate the highest electric output compare with other substrate materials

The performance of the piezoelectric cantilever beam (PZT-5J and structure steel) of the EH device and its eigenfrequency are shown in Figure 22.

The Eigenfrequency of cantilever beam has been studied and analysed by COMSOL Multiphysics And it is 21.6 Hz.

The cantilever beam of EH device has low eigenfrequency. Based on that, it can response to the low wind flow velocity and human motion acceleration.

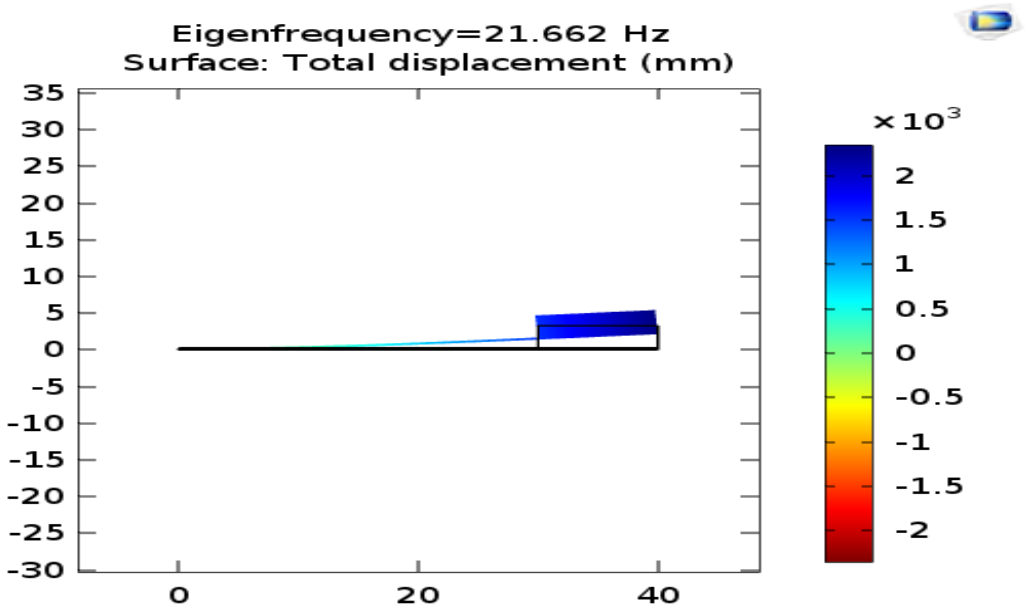

Figure 22. Eigenfrequency of cantilever piezoelectric beam

2.5. Possible vibration sources for EH device

Mechanical energy can be harvested through vibration. The two main components of vibration are frequency and peak acceleration. Kin et al. [19] summarize the potential sources of vibration in Table 7.

Table 7. Vibration sources [19]

Human Body	Vehicles	Structure	Industrial	Environment
Walking, arm motion, finger motion, swimming, running, eating, talking	Aircraft, unmanned air vehicle, helicopter, automobiles, trains	Bridges, roads, tunnels, farmhouse structures	Motors, compressors, chillers, pumps, fans	Wind, solar, temperature gradient, daily temperature
Breathing, blood pressure, exhalation, body heat	Tiers, tracks, peddles, brakes, shock absorbers, turbines	Control switch, heating, ventilation and air conditioning systems, ducts, cleaners	Conveyors, cutting and dicing, vibrating machines	Ocean currents, acoustic waves, electromagnetic waves, radio frequency signals

The conversion of vibration to electrical power is not suitable for all environments. In order to maximize the potential suitability of the project, the vibration sources should be relatively low in frequency below 200 Hz [20]. S. J. Roundy lists vibration sources with low frequency, as given in in Table 8.

Table 8. Vibration sources that have frequency less than 200 Hz [20]

Vibration Source	Peak Acc. (m/s^2)	Frequency of peak (Hz)
Kitchen blender casing	6.4	121
Clothes dryer	3.5	121
Door frame just after door closes	3	125
Small microwave oven	2.25	121
HVAC vents in an office building	0.2–1.5	60
Wooden deck with people walking	1.3	385
Notebook computer while CD is being read	0.6	75
Washing machine	0.5	109
Bread-maker	1.03	121
Human motion	1.3	-

The cantilever beam structure is utilized in specific dimensions and with an appropriate piezoelectric material to construct the piezoelectric transducer with a low resonant frequency of 21.6 Hz to customize it to the low wind velocity flow and the vibration of human motion. The vibration sources in this research are wind flow (between 1 and 20 m/s) and human motion acceleration (1.3 m/s^2) [21].

3. Evaluation of the prototype design

Wind flow is caused by the difference in the pressure levels between two points; the flow takes place from an area of high pressure to an area of low pressure. [22]

There are two types of flow laminar and turbulent. In laminar flow, the fluid flows through the pipe or tube smoothly or in a regular path. In turbulent flow, fluids have irregular paths and show irregular fluctuations. [22]

Simulation of air flow can be done by ANSYS CFD to study the behaviour of the wind flow through a pipe or tube and to predict the patterns.

The portable EH device can be used by runners and skiers to generate electric output power through their motions. The shape of this device plays an important role in gathering the wind at the inlet and increasing the velocity of the wind at the outlet. Also, the generated electric power depends on the acceleration of human motion.

Several shapes are studied to develop a shape that gives the best results. The material of the shape has to be plastic. The advantages of using plastic are that it is lightweight and can be easily modelled and strengthened. [23]

3.1. The first prototype design

The first prototype is the tube (150 mm × 50 mm × 50 mm). At the outlet of this tube, there is a cantilever beam of piezoelectric material which is fixed at one side, as presented in Figure 23 (Appendix 2).

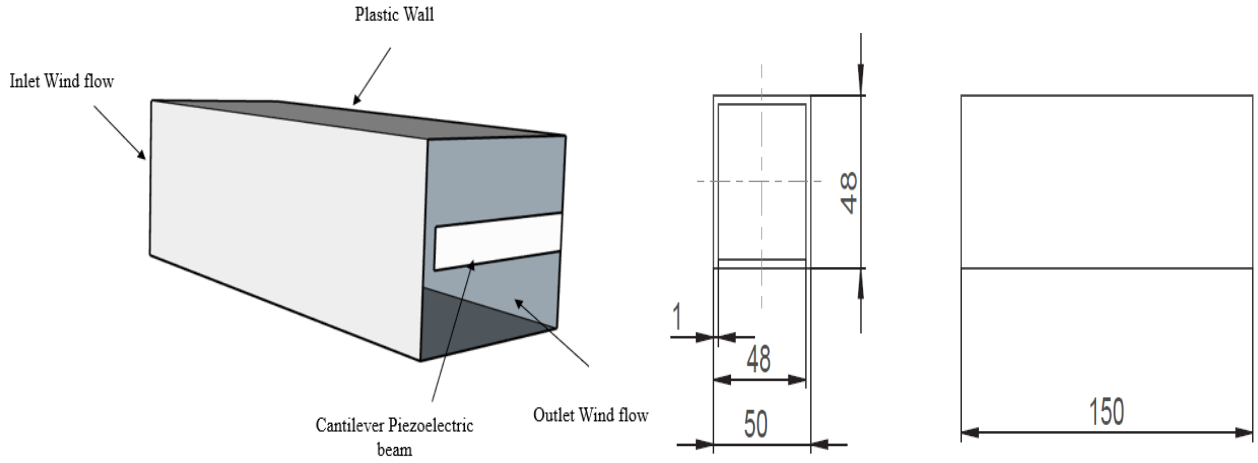

Figure 23. Design of tube prototype

The velocity streamline is presented in Figure 24. The velocity is high at the outlet because the offset at the frame changes the path of the air, which cannot go straight and must take a curved path to reach the outlet.

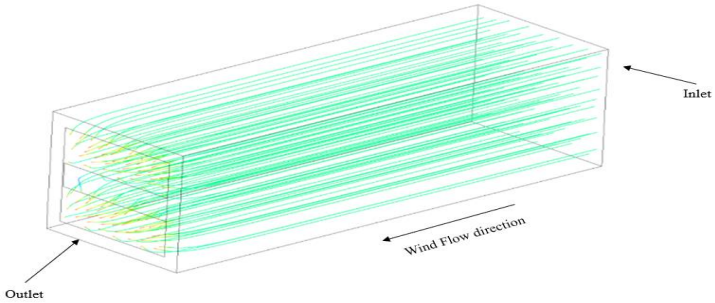

Figure 24. Streamline of wind flow through the tube prototype

When the wind is hit by a surface, the dynamic energy of the wind is transformed to pressure. This pressure, when acting on the surface, transforms into force.

Table 9 shows the input velocity, output velocity, and force load result from wind flow. These results are calculated by ANSYS CFD.

Table 9. Results of velocity, pressure, and force of tube prototype

Input Velocity, m/s	Output Velocity, m/s	Pressure in Piezo, Pa	Force, N
1	4.26735	10.90	0.00437
2	6.46544	25.10	0.0100
3	8.67813	45.20	0.0181
4	10.8918	71.20	0.0285
5	13.1073	103.0	0.0412
6	15.3254	141.0	0.0564
7	17.5445	185.0	0.0739
8	19.7639	234.0	0.0937
9	21.9836	290.0	0.12
10	24.2039	351.0	0.14
11	26.4243	419.0	0.17
12	28.6448	492.0	0.20
13	30.8655	572.0	0.23
14	33.0864	6570	0.26
15	35.3071	748.0	0.30
16	37.5280	845.0	0.34
17	39.7491	948.0	0.38
18	41.9702	1057	0.42
19	44.1915	1172	0.47
20	46.4128	1292	0.52

Figure 25 illustrates a plot of the output electric power over a range of frequencies between 17 and 27 Hz. The maximum power (82.6 mW) occurs at the eigenfrequency of 22.8. The piezoelectric transducer generates high power when vibrating at its resonance frequency.

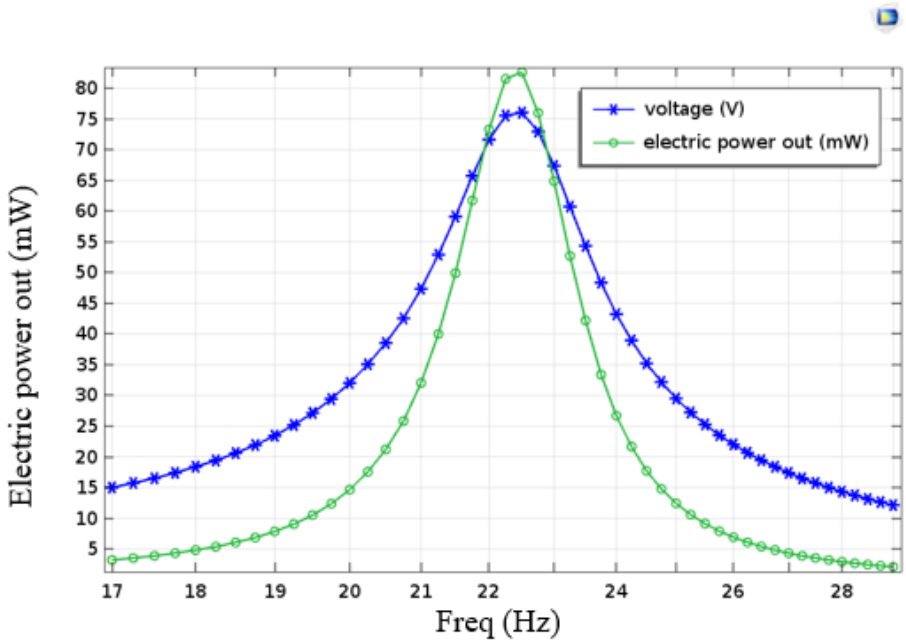

Figure 25. Performance of electric output power as a function of the eigenfrequency of the tube prototype

The electric output power increases when the external force related to the acceleration of wind flow and human motion is larger. Human acceleration is 1.3 m/s^2 and the wind flow velocity range is 1–20 m/s. Figure 26 shows the relation between the electric output power and the external force.

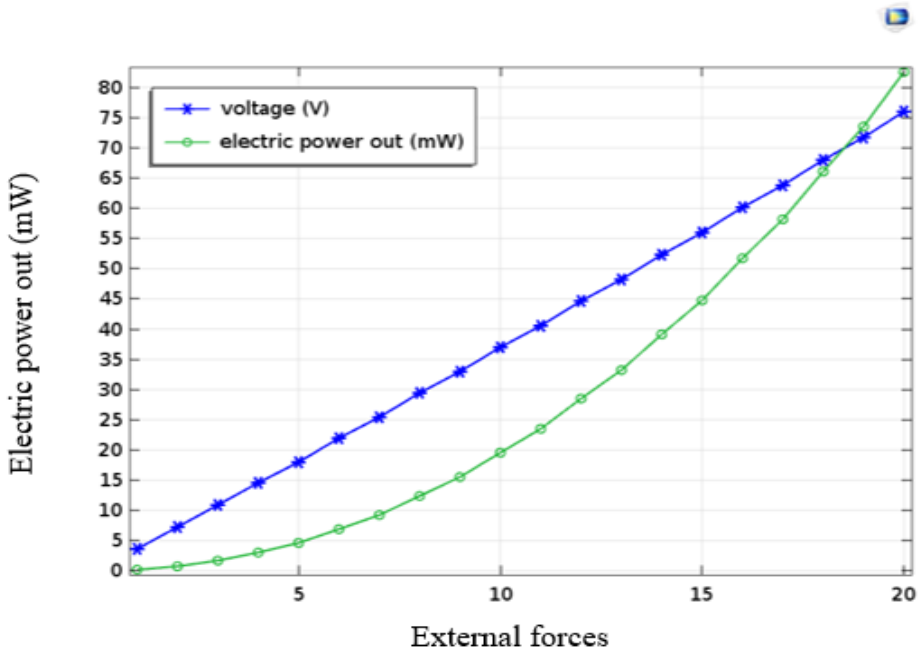

Figure 26. Relation between electric power output and external force in the tube prototype

The generated electric power is between 1 and 82.6 mW, as shown in Figure 26.

3.2. The second prototype design

The second prototype design is the cylinder (150 mm × 51 mm) with a fixed piezoelectric beam at one side of the outlet.

This design is supposed to give better output velocity because of its smooth walls. The design and the dimension are presented in Figure 27 (Appendix 3).

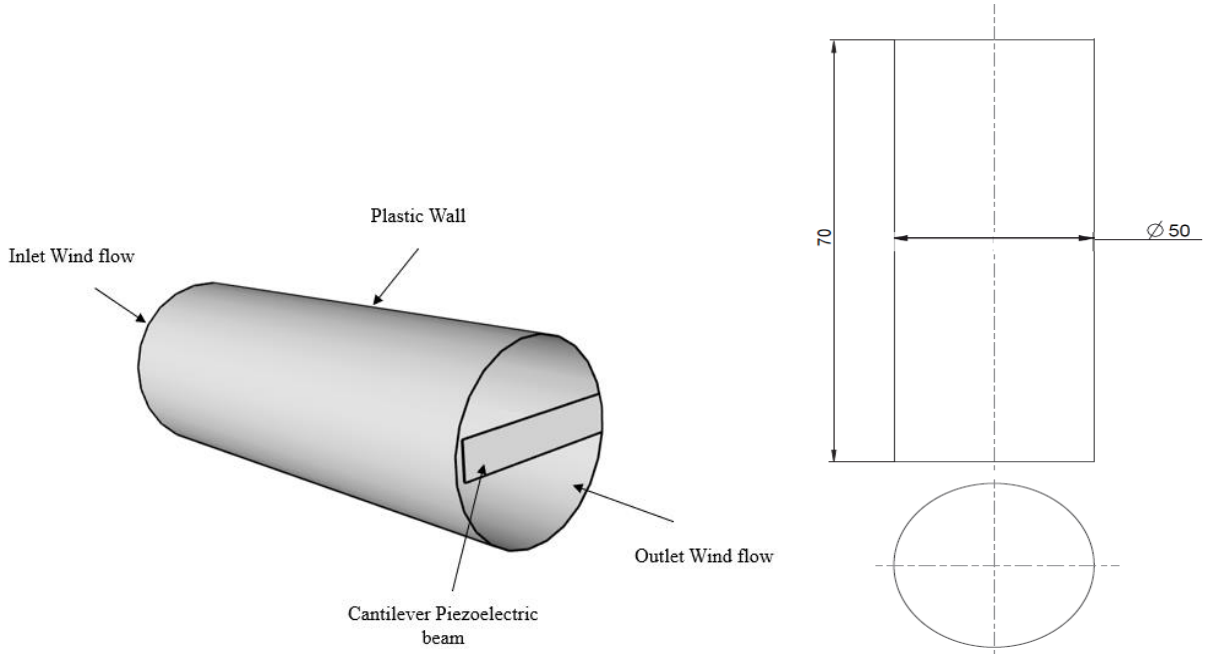

Figure 27. Design of cylinder prototype

The streamline given in Figure 28 shows the wind flow from the inlet to the outlet. The path of the wind flow changes direction because of the offset at the frame near the outlet.

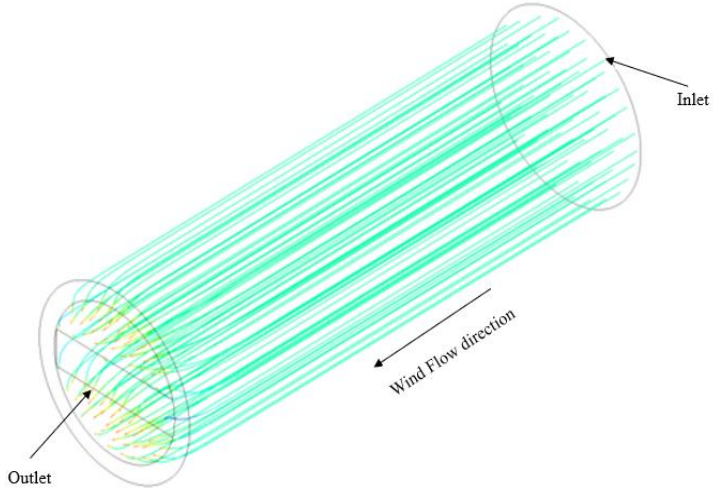

Figure 28. Streamline of air flow through the cylinder prototype

The wind flow performance is simulated by ANSYS CFD. The outlet velocity is used to calculate the force load of wind flow. The results are presented in Table 10

Table 10. Results of velocity, pressure, and force of cylinder prototype

Inlet Velocity, m/s	Outlet Velocity, m/s	Pressure in Piezo, Pa	Force, N
1	4.8735	11.50	0.005
2	6.76544	25.90	0.012
3	8.97813	46.20	0.021
4	10.9918	72.20	0.032
5	13.2073	104.0	0.042
6	15.8254	143.0	0.061
7	17.6445	187.0	0.082
8	18.8772	237.0	0.112
9	20.1112	293.0	0.153
10	24.3458	356.0	0.181
11	26.5812	424.0	0.212
12	27.8171	498.0	0.251
13	30.0535	579.0	0.303
14	33.2903	665.0	0.351
15	37.5276	757.0	0.373
16	40.765	856.0	0.411
17	43.0027	960.0	0.462
18	46.2408	1071	0.491
19	48.4791	1187	0.542
20	50.7177	1310	0.581

The results, as shown in Table 9, indicate that the second design of shape is better than the first design; the outlet velocity of the cylindrical shape is higher than that of the tube shape. This means that more force load is applied on the piezoelectric cantilever beam.

The forces of wind flow resulted from ANSYS CFD and the acceleration of human motion used in COMSOL Multiphysics to study the electric output in different cases such as the relation between the eigenfrequency and electric output, and the relation between the relation between the external forces and electric output.

The following figures described all the results of electric output. In this research, the same piezoelectric cantilever beam is used. Based on this, Figure 29 shows that the electric output power is the maximum of 84.1 mW at the eigenfrequency of the cantilever beam of 23.8 Hz.

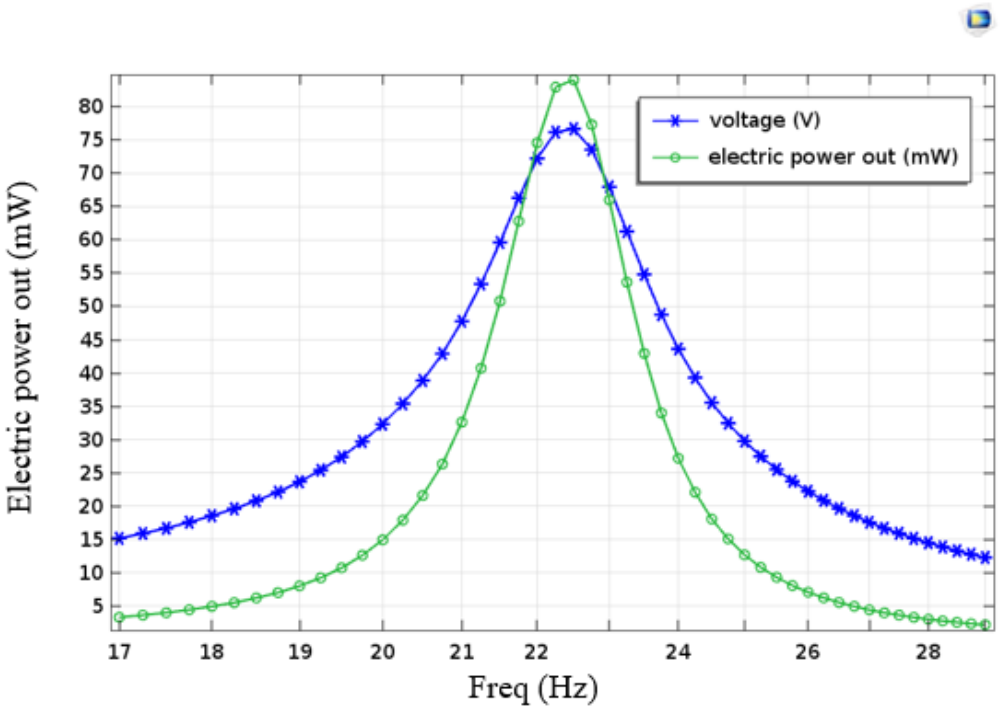

Figure 29. Performance of electric output power as a function of eigenfrequency of the cylinder prototype

Figure 30 shows the relation between the electric output power and the external force (wind flow and human motion). The electric output power increases when the external force is larger.

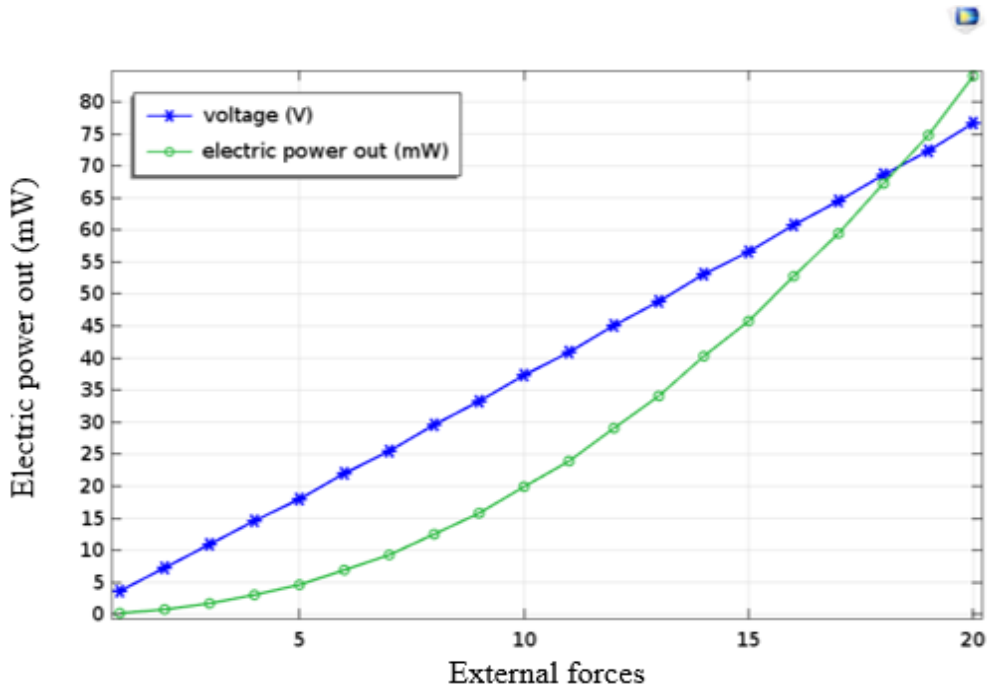

Figure 30. The relation between electric power output and external force in the cylinder prototype

The generated electric output power range is 1.5–84.1 mW in relation to the increase in external forces. The results show that the cylindrical design is better than the tube design. The outlet velocity of the cylindrical design is higher than that of the tube design. This means that the cylindrical design generates more electric output power.

3.3. The third prototype design

The third design of prototype is the cylinder (150 mm × 51 mm) with a narrow midsection. There is a cantilever piezoelectric beam at the outlet.

The cylinder with a narrow midsection is designed to increase the output velocity of wind flow, as shown in Figure 31 (Appendix 4).

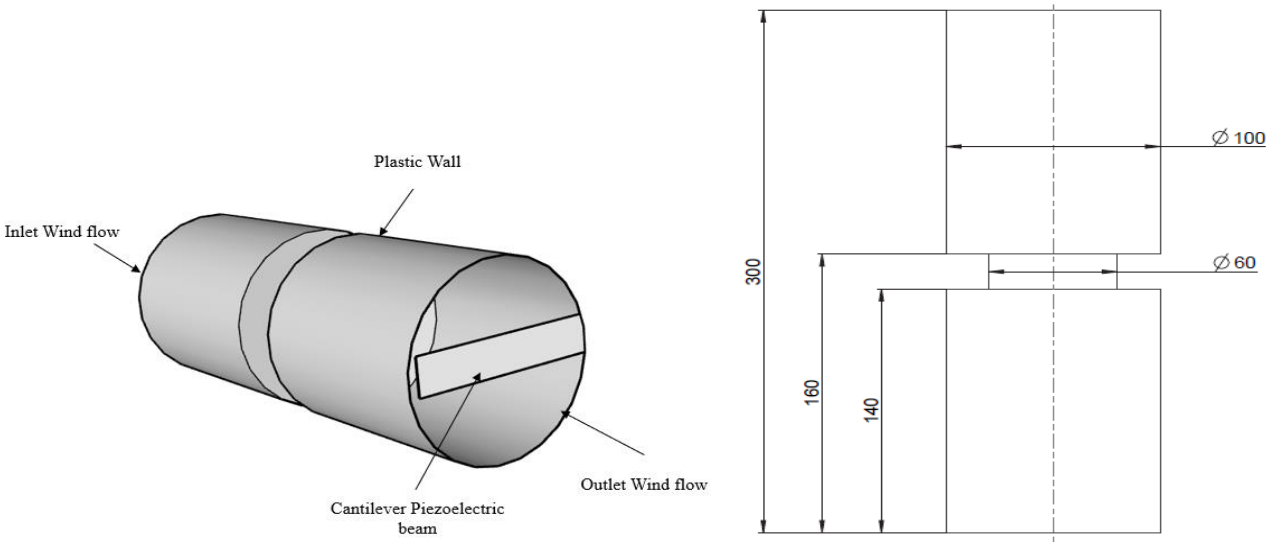

Figure 31. Design of cylinder with narrow midsection prototype

The streamline in Figure 32 shows the flow of the air from the inlet to the outlet. The outlet velocity increases because of the offset at the middle and at the frame of the outlet.

These two offsets change the pressure through the cylinder twice once in the middle and once at the outlet. According to the relation between the velocity and pressure, the outlet velocity increases.

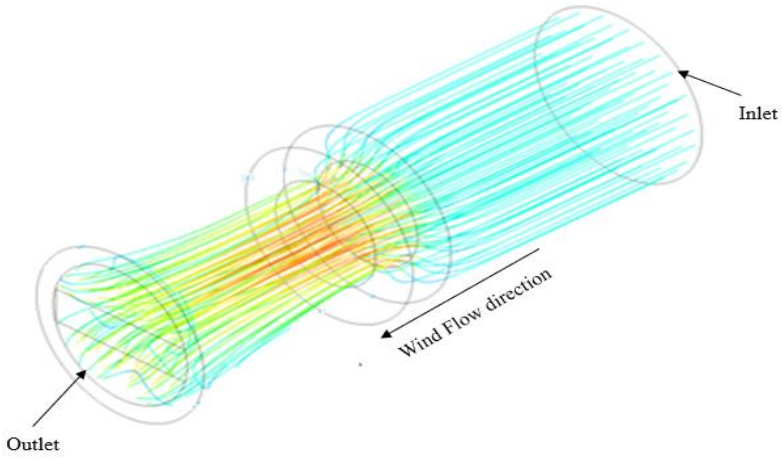

Figure 32. Streamline of air flow through the cylinder with narrow midsection prototype

The output velocity and pressure are measured by ANSYS CFD. After that, the force load of wind flow is calculated. Table 11 shows the results

Table 11. Results of velocity, pressure, and force of cylinder with narrow midsection prototype

Inlet Velocity, m/s	Outlet Velocity, m/s	Pressure in Piezo, Pa	Force, N
1	5.22531	16.4	0.00655
2	7.94437	37.9	0.0151
3	10.7309	69.1	0.0276
4	13.2828	106	0.0434
5	15.9773	153	0.0613
6	19.1101	219	0.0876
7	21.3839	274	0.11
8	23.6733	336	0.13
9	27.1721	443	0.18
10	30.1879	547	0.22
11	32.48	633	0.25
12	34.9578	733	0.29
13	38.5671	892	0.36
14	41.0651	1012	0.4
15	43.8613	1154	0.46
16	45.001	1215	0.49
17	48.5187	1412	0.56
18	50.8653	1552	0.62
19	52.8458	1676	0.67
20	55.2725	1833	0.73

Further analysis shows that the third shape design a cylinder with narrow midsection increases the outlet velocity more than other two shape designs

The forces of wind flow resulted from ANSYS CFD and the acceleration of human motion used in COMSOL Multiphysics to study the electric output in different cases such as the relation between the eigenfrequency and electric output, and the relation between the relation between the external forces and electric output.

The generated electric power is maximum at the eigenfrequency of the cantilever beam at 87.8 mW. This means that this design gives the best electric output at the same eigenfrequency as the other designs.

Figure 33 presents the generated electric output as a function of the eigenfrequency.

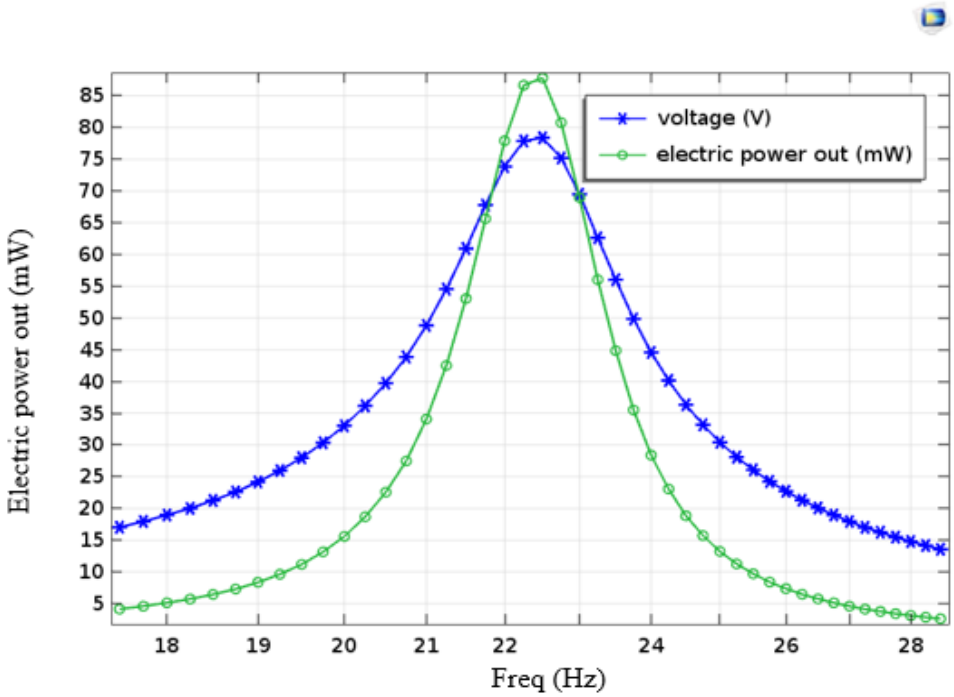

Figure 33. Performance of electric output power as a function of the eigenfrequency of the cylinder with narrow midsection prototype

Figure 34 illustrates the relation between the generated electric power and the external forces. As mentioned before, the external forces are the wind flow of 1–20 m/s and human motion.

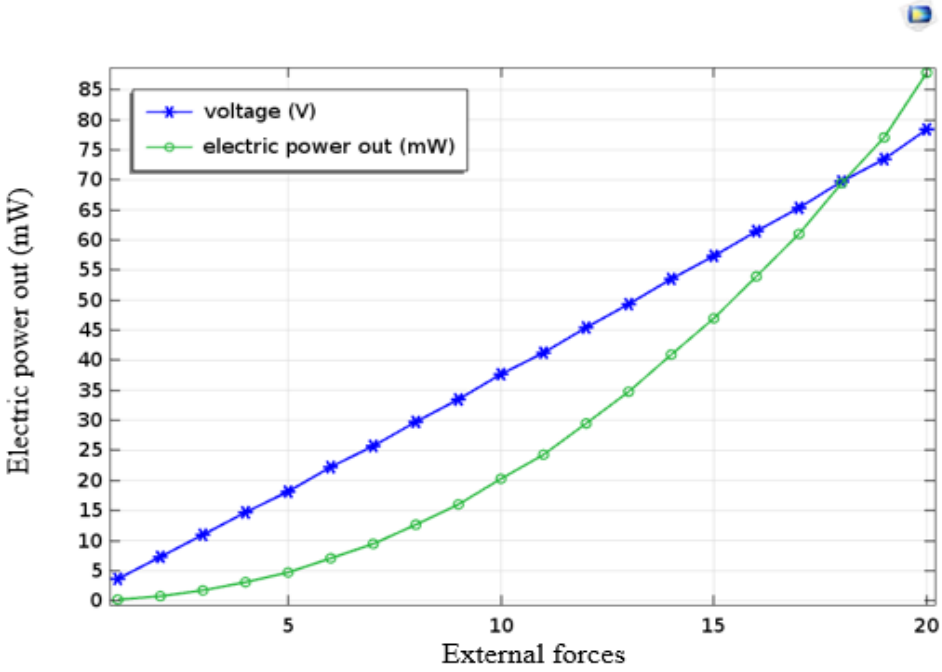

Figure 34. The generated electric power as a function of the external force in the cylinder with narrow midsection prototype

The results of the electric output power were between 2 and 87.8 mW

The harvester is excited at its eigenfrequency 22.8 Hz, under the external load of 20 m/s and human motion acceleration of 1.3.m/s^2. The electric output power can be obtained as a function of the load resistance. Figure 35 shows the relation between the output power and load resistance.

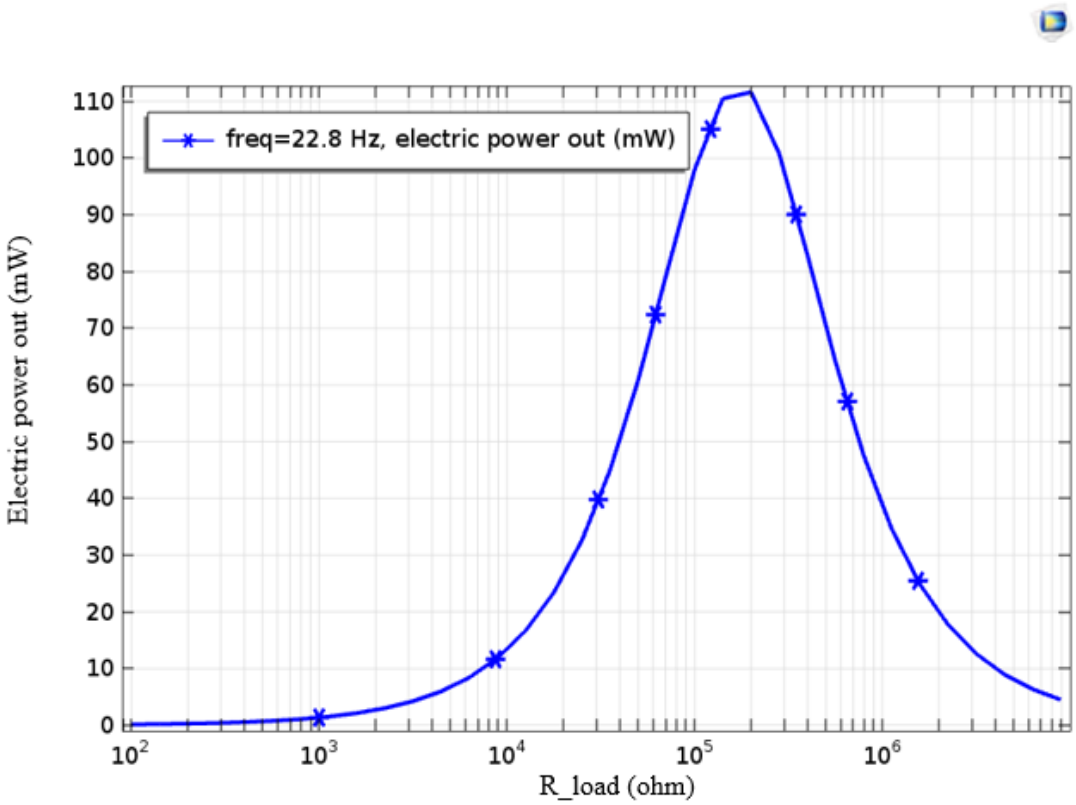

Figure 35. The generated electric power as a function of the load resistance

It is clear that the generated electric power is highly dependent on the electric resistance. The generated power increases on increasing the load resistance until it reaches its peak.

The wind flow and the acceleration of human motion are the external forces that excite the cantilever piezoelectric beam to generate electric power. The shape of harvester plays a vital role in increasing the output velocity.

Three different designs are simulated and studied precisely to determine the best shape design to yield the highest output velocity. The best design is a cylinder with narrow midsection because its output velocity is higher than that of the other two designs.

Figure 36 shows a comparison of the electric output power of the three prototype designs and the maximum generated power recorded in the cylinder with narrow midsection.

The three prototypes have been compared according to their electric output, and it is done by COMSOL Multiphysics to study the behaviour of cantilever beam under the external forces.

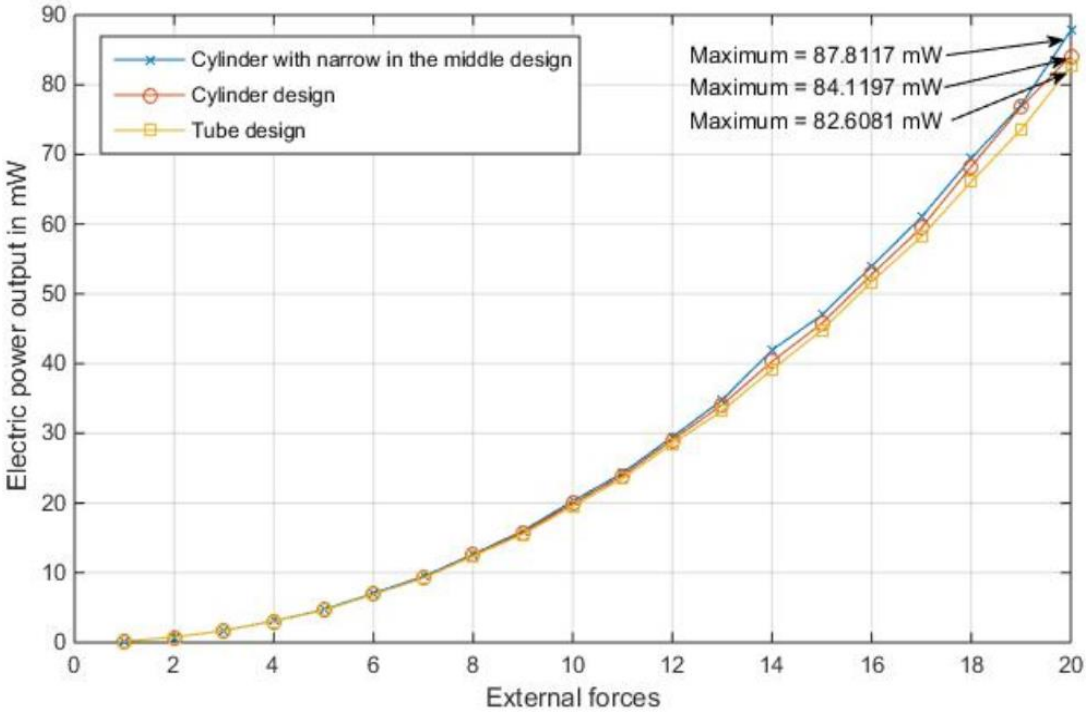

Figure 36. Comparison of the electric output power of the three designs

Through simulation study, the three prototype designs are compared for power generation under the same external force excitation. It is found that the prototype design of the cylinder with narrow midsection outperforms the other prototype designs. Based on this, the prototype with narrow midsection is the design used for the EH device.

4. The control unit of energy harvesting device

The EH device usually has varied output voltages and polarities. Sometimes, the generated voltage is too low or too high for the application. The main task of power management (PM) is to rectify the output voltage and match the output voltage with the impedance of the device.

Therefore, the PM circuit plays an important role in the system. Figure 37 illustrates the main components of the PM circuit.

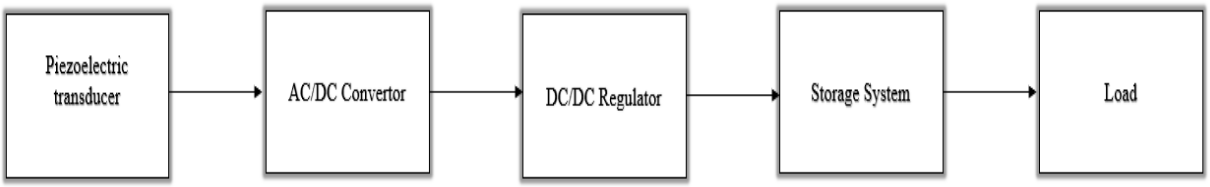

Figure 37. PM Circuit Components

The components of PM circuit are an AC-DC converter, a voltage regulator, and an energy-storing device, which perform the following functions:

- Converting the AC voltage output from the piezoelectric transducer to direct current (DC)
- Regulating the DC power supplied to the external load or the storage device
- Storage device: storing the harvested energy

The voltage and the current generated from the piezoelectric material are changeable. The converter is the essential component to produce DC for power supply. Additionally, the regulator is important when the generated voltage has a large amplitude and frequency fluctuation.

The control unit of energy harvesting device should design it accurately to keep the generated voltage high and reduce the losses between the components.

4.1. AC-DC Rectifier

Full-Wave Rectifying Circuit

Full-wave rectifier is a circuit that makes use of both half-cycles of input AC and converts them to DC.

The full-wave rectifier consists of four diodes (D1, D2, D3, D4) arranged together to form a bridge. The secondary transformer is connected to two opposite points of the bridge and the load resistance R is connected to the bridge. The AC supply is applied to the circuit through the transformer.

The schematic of the circuit is presented in Figure 38 [24].

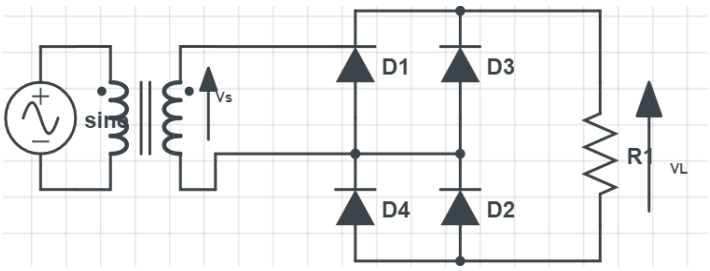

Figure 38. Full-Wave Rectifier

In Figure 39, the waveform of a full-wave rectifier is shown.

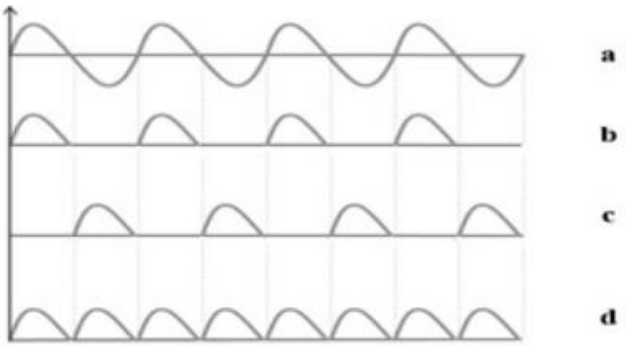

Figure 39. Waveforms [25]

The first waveform (a) represents the input AC signal, the second (b) and the third (c) waveforms are the DC current generated from D1 and D2 respectively. The fourth waveform is the total output DC current.

The output DC voltage is calculated at the load resistor R by [25]:

$$V_{DC} = \frac{2V_{max}}{\pi} \quad (6)$$

V_{DC}- the output DC voltage; V_{max}-maximum secondary.

This AC/DC rectifier is a part of the control unit circuit of the EH device because of its advantage namely low power loss since both half-cycles are converted.

4.2. DC regulator

DC regulator is used if the generated voltage is less or higher than the required voltage and needs to be brought up or down to be appropriate and useful for the target application or storage system. The problem with EH is that the generated energy level is in the millivolt range. In light of that, the DC regulator should convert the voltage with small losses.

Buck and boost converters

Buck converters produce lower output voltage than input voltage. Such regulators fit high-voltage EH transducers [26].

Boost converters produce higher output voltage than input voltage. Such regulators fit the low-voltage EH transducers.

These two converters are created by the principle of charging and discharging an inductor through a transistor.

The buck and boost converters have limitations; they cannot be used with different EH transducers because each works in one mode bucking or boosting the input voltage. Also, it is difficult to control them.

Buck-Boost converter

A buck-boost converter combines the principles of both a buck converter and a boost converter in one circuit [27].

This converter receives an input DC voltage and produces an output voltage at different levels, either lowering or boosting the voltage as required by the application.

It is created by the same principle as the buck and boost converters an inductor being charged or discharged through a transistor to control the voltage.

The advantage of a buck-boost converter is that it works in two modes bucking and boosting the output voltage because it combines two convertors buck and boost.

IC Chip: Power Management Integrated Circuit (PMIC)

The PMIC is commonly used in the EH system. It can convert the unstable input into regulated current to be used in different applications and storage systems.

Moreover, one of the most important features of PMIC is the ability to protect the storage system by avoiding overcharging and being fully empty.

The critical issues of the PMIC that should be considered during its selection are small chips, high efficiency, and low power consumption.

The selected PIMC is BQ25570 by Texas Instrument (Appendix 5). This chip has lower power consumption compared to other products; it consumes 488 nA. BQ25570 is shown with pin names in Figure 40.
The body size of BQ25570 is considered small (3.50 mm × 3.50 mm). based on that, BQ25570 is appropriate chip for portable device because of its size and properties.

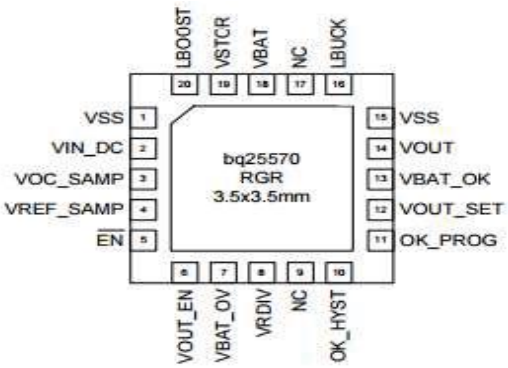

Figure 40. BQ25570 chip with pin names [28]

Additionally, the threshold level of charge and discharge can be determined; this feature can protect the storage system, as mentioned before.

The external resistors R_{ok1}, R_{ok2} determine the V_{BAT}_oV threshold level according to the following equation: [28]

$$V_{BAT}\_oV = \frac{3}{2} VBIAS \left(1 + \frac{R_{ok2}}{R_{ok1}}\right) \quad (7)$$

VBIAS is the internal reference for the programmable voltage thresholds.

The external resistors R_{out1}, R_{out2} determine the V_{out} output voltage according to the following equation: [28]

$$V_{out} = VBIAS\left(\frac{R_{out2}+R_{out1}}{R_{out1}}\right) \quad (8)$$

The IC consists of a buck controller at the inlet and a boost controller at the outlet. The buck controller brings down the voltage for the piezoelectric cantilever beam if needed, while the boost controller brings up the voltage to a regulated voltage at the output.

In general, therefore, it seems that the BQ25570 is the appropriate IC chip for this study because of its advantages of combining two DC convertors, protecting the storage system, and consuming less power.

4.3. Storage system

The output voltage EH device is low; thus, the output power cannot be used directly by an electronic device.

The solution to this problem is to accumulate the output power in a storage system before it is used by the sensors.

The storage systems for EH devices are capacitors or rechargeable batteries.

4.3.1. Capacitors

A capacitor has two conductive electrodes separated by a dielectric, which means that no current flows through the material during charging. The main task of the dielectric is to produce an electric field to allow the capacitor to store energy.

Capacitors require rapid energy transfer; they are not considered as a suitable storage for applications that require stable and steady energy.

Supercapacitors are of three different types electric double-layered capacitors, pseudo-capacitors, and hybrid capacitors. Electric double-layered capacitors, the most commonly used capacitors, are shown in Figure 41 [29].

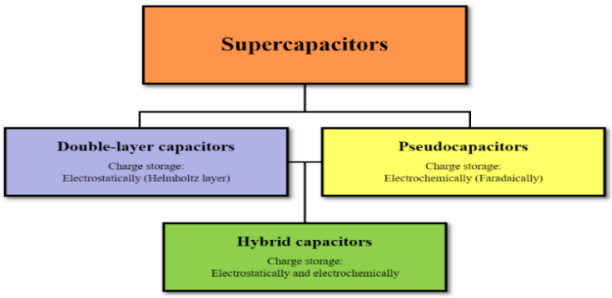

Figure 41. Supercapacitor types [29]

The advantage of using capacitors is that they do not require a minimum voltage to begin charging. Also, they can charge and discharge quickly and can provide accumulated power directly to the electronic device.

On the downside, capacitors have lower power density compared to batteries.

Double-layered capacitors

This capacitor consists of two carbon electrodes. Figure 42 is a general schematic of the typical double-layered capacitor [30].

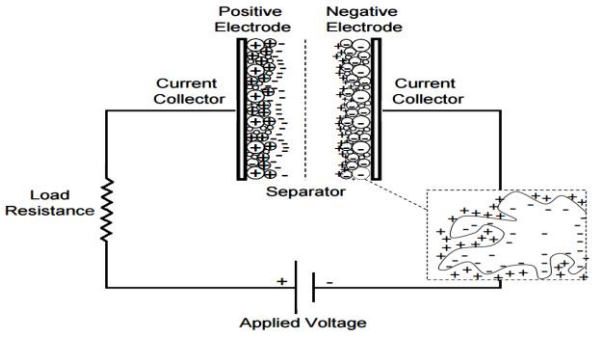

Figure 42. Double-layer capacitor [30]

When voltage is applied to the carbon electrodes, an electric field is created between the charged electrodes, making the charged ions in the electrolyte migrate towards the electrodes of opposite polarity.

Pseudo-Capacitors

This capacitor consists of two polymers or metal oxide electrodes, which are separated by an electrolyte [28]

The advantages of using pseudo-capacitors are their high capacity and low price.
On the downside, the lifetime of this capacitor is shortened if a mechanical stress is applied during charge and discharge.

Hybrid capacitors

Hybrid capacitor is the combination of a double-layered capacitor and a pseudo-capacitor. The hybridization helps to combine the advantages of the two types of capacitors and tries to extenuate the disadvantages [31].

The disadvantages of using a capacitor in an EH device is that the amount of energy stored is considerably lower than in case of a battery.

4.3.2. Batteries

A battery is an electrochemical cell with three main components a negative electrode (anode), a positive electrode (cathode), and a chemical material (electrolyte) between them.

Batteries are divided into two categories batteries with an irreversible chemical process and those with a reversible chemical process. All these batteries are rechargeable [32].

The electrons in the anode result in the interaction between the ions and the atoms. In general, the anode is negative and the cathode is positive. The electrolyte acts as a barrier to prevent the electron from flowing from the anode to the cathode.

The only way to let the electron flow from the anode to the cathode is to create a closed circuit.

In general, the voltage generated from an electrochemical cell is determined by several criteria, such as the ability of the anode to send out electrons and the ability of the cathode to attract electrons.

This ability is called standard electrode potential; its symbol is E^0 Volt.

$$E^0_{cell} = E^0_{cathode} - E^0_{anode} \quad (9)$$

Table 12 presents the main standard electrodes used in manufacturing batteries. These reactions take place during the charging phase and are reversed during the discharge phase.

Table 12. Standard battery electrode [33]

Battery	Reactions	E^0(V)
H	$2H^+ + 2e^- \rightarrow H^2$	0
Li	$Li^+ + e^- \rightarrow Li(s)$	−3.05
Ni-Cd (cathode)	$2NiOOH + 2H_2O + 2e^- \rightarrow 2Ni(OH)_2 + 2OH^-$	+0.48
Lead-Acid (anode)	$PbSO_4 + 2e^- \rightarrow Pb + SO^{2-}_4$	−0.35

Lithium batteries

According to Table 1, lithium has the highest reduction potential, which is why lithium is one of the most favourable materials for producing rechargeable batteries.

The working principle of lithium-ion batteries is based on the flow of positive lithium ions through an electrode while an external circuit is connected to the anode and cathode [34].

During the charge phase, an external voltage is applied to the battery cell. Lithium ions start to flow from the positive electrode through the electrolyte and intercalate between the graphite sheets, thus increasing the potential energy of the lithium ions.

During the discharge phase, electrons starts to flow in the external circuit from the negative electrode to the positive one due to the potential difference and electric field.

One of the main limitations is the limited number of charge/discharge cycles. When the cell is charged for the first time, the electrolyte makes a film around the graphite, which functions as a layer that is permeable for lithium ions but non-permeable for electrons [34]. This layer is essential for the functioning of the cell, but it grows thicker over time and leads to increased internal resistance of the cell. The new technology of lithium battery increases the number of charge and discharge cycles to 5,000 full cycles. It is produced by TLI lithium battery. This kind of battery is produced specially to fit EH applications [35].

The storage solution of this work is a lithium battery by TLI lithium battery. The charge voltage is 4.1 V and the capacity is 140 mAh. Additionally, the advantages of this battery are the long operation life of around 5,000 full cycles and wide operating temperature range. The life cycle of storage unit is one of the most important criteria when choosing the storage system for energy harvesting device.

Summary of the control unit

PM plays a vital role in enhancing the output of an EH device. As mentioned above, the first step of PM is AC/DC transformation—it is considered as an important step to convert the voltage from AC to DC. Then, DC/DC regulation is used to get an output with constant voltage. The aim of these steps is to get constant voltage, which should suit the storage system.
The overall scheme of the electronic unit of the EH device is shown in Figure 43.

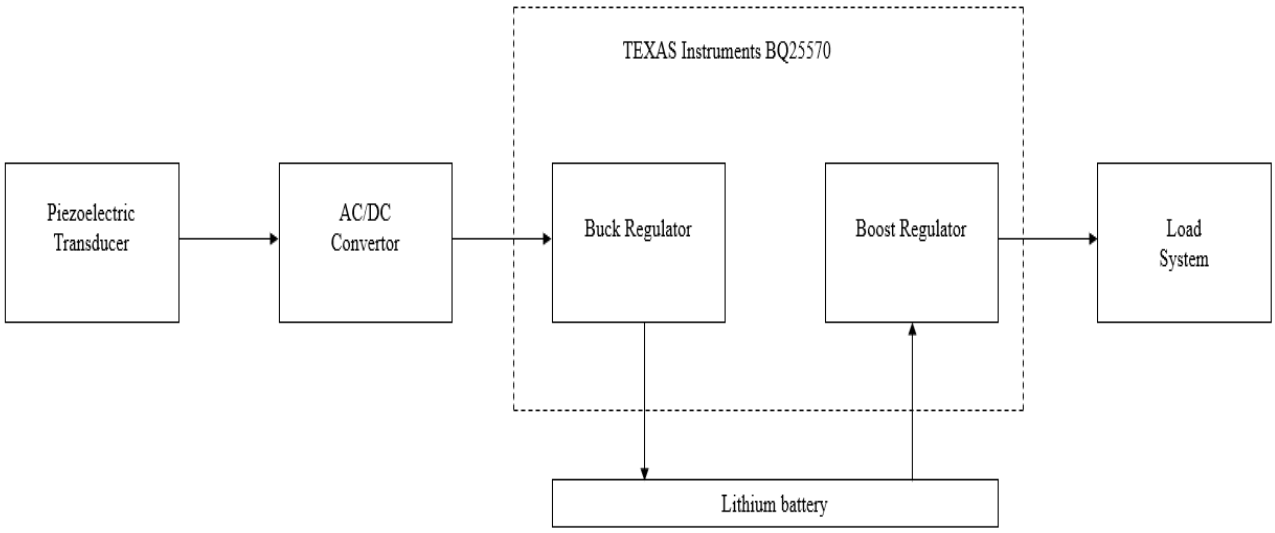

Figure 43. Electric unit of EH device

The algorithm flowchart of the EH device describes the step-by-step working principle, from the vibration of wind flow and human motion to the storage of the generated power in the lithium battery (Figure 44). Firstly, the vibration is initiated by the wind flow and the human motion. Likewise, the vibration is examined to check if it is enough to generate AC voltage.

The AC voltage generated from piezoelectric material is converted to DC voltage by AC/DC convertor.

After that, the DC voltage transferred to BQ25570 to regulate the DC voltage and charge the battery. In addition, by BQ25570 provide feedback to check the capacity of battery to protect it from over charging.

In summary, it is electricity production process that starts from vibration of piezoelectric material to the end of power storage.

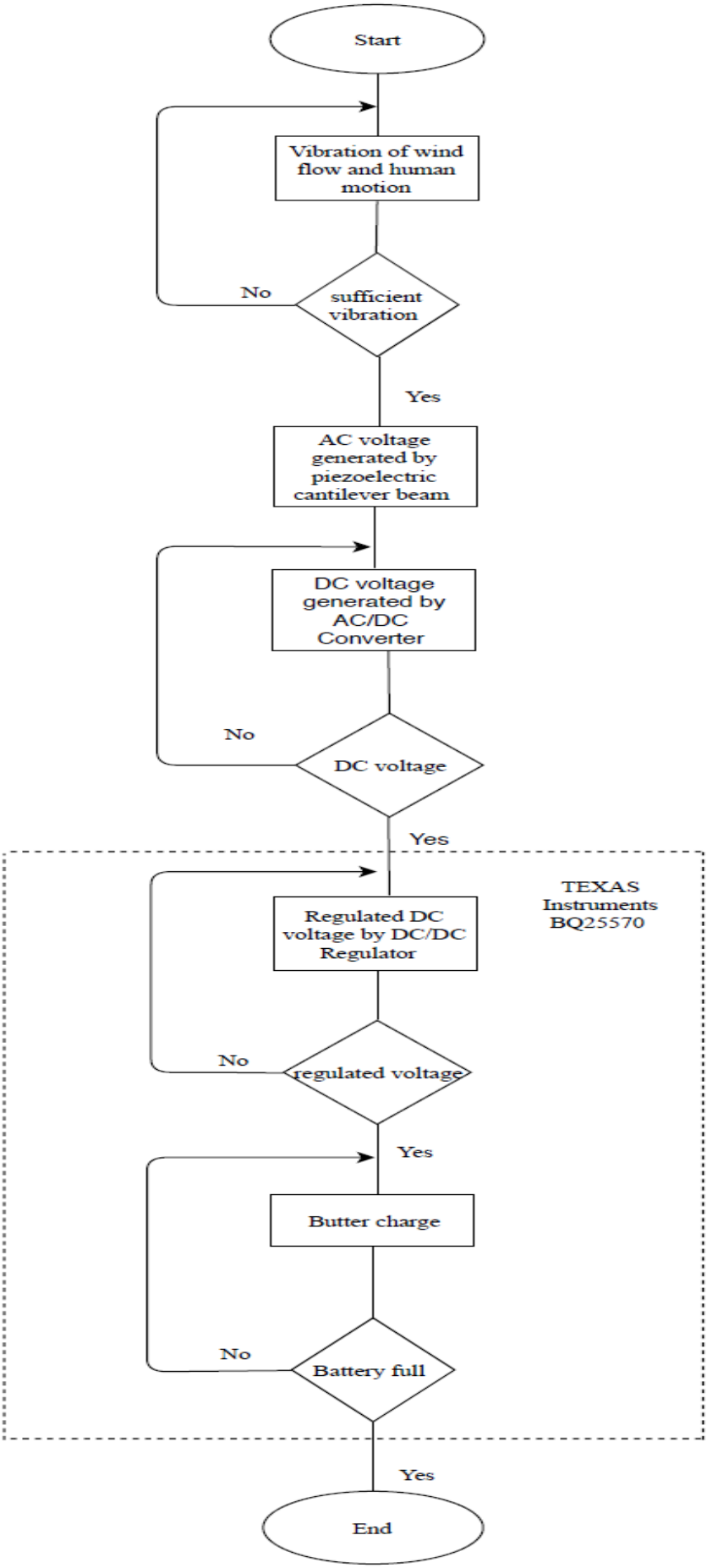

Figure 44. Algorithm flowchart of EH device operation

5. The design of the portable device

The EH device could be used as a portable device by walkers. The small size allows the users to use the device in several forms, such as hand-held device, attached to a bag, or attached to the shoulder of walkers.

The EH device consists of three main components a cylinder with narrow midsection which gives the direction of wind flow, a control unit to regulate the output voltage generated by the designed beam of piezoelectric material, and a lithium battery to store the electric output power. Figure 45 shows the parts of the EH device.

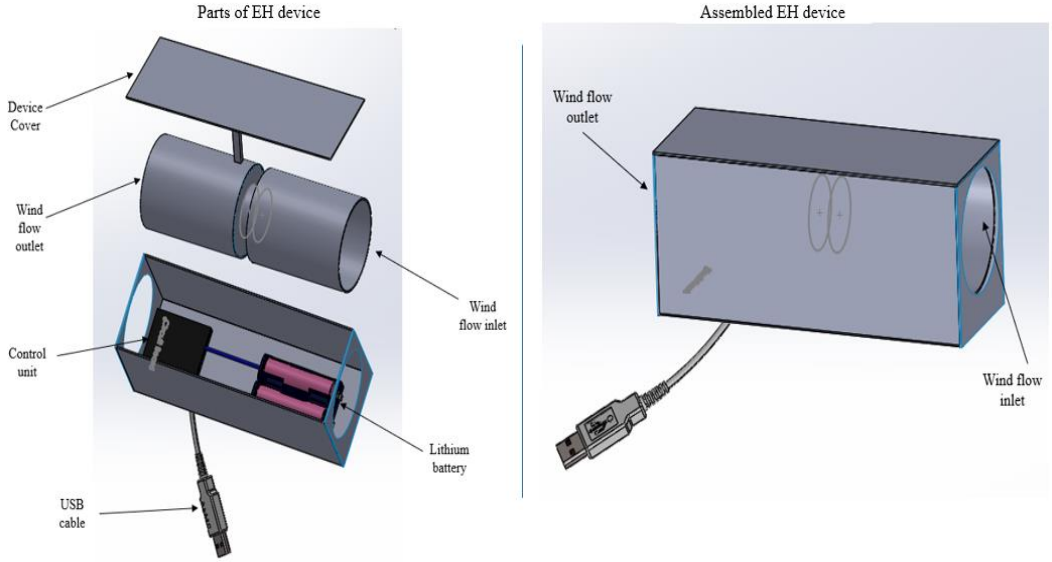

Figure 45. The EH device

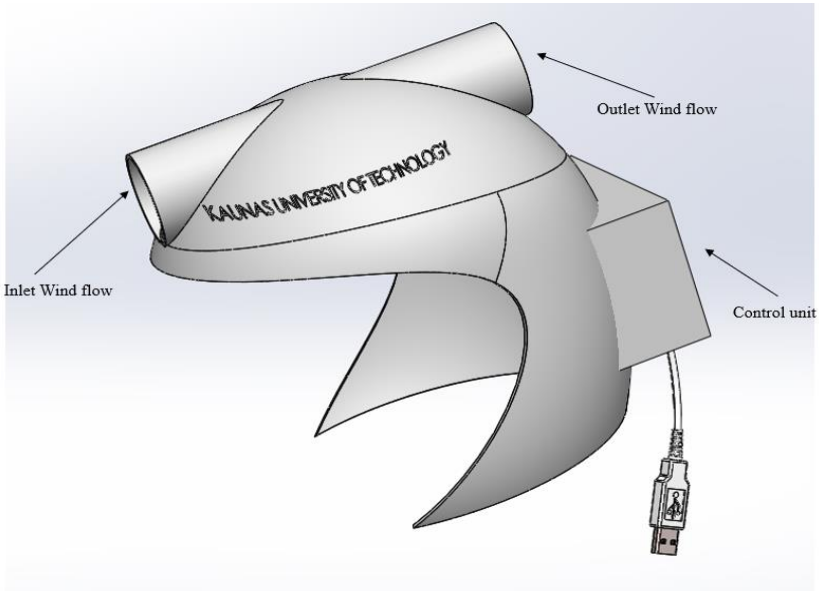

Figure 46. EH helmet

The proposed portable energy harvesting device developed to be easily handled by walkers and it is a small form of a computing device that is designed to be held or attached with another device or the body of walkers to generate electricity during their motion.

Another form of EH device can be attached to the helmet of special walkers. It doubles up as a protective device and an EH device. It is presented in Figure 46.

Special walkers can use the helmet to generate electricity during their motion, this helmet is not only EH device it is also protective device.
This helmet can be used in many applications that are exposed to outdoor activities. The power supply is a compact unit comprising the piezoelectric cantilever beam, control unit and lithium battery.

Conclusions and suggestions

This MA project focuses on the development of a portable EH device that can be used as a handle device by walkers, allowing them to generate energy during motion.

The energy harvesting device has been developed to generate electric power from wind flow with human motion and then regulate the output voltage to transfer the generated energy to the storage system.

The energy harvesting device has been developed for use in several forms for example, as a hand-held device or as a helmet for skiers.

The main goals of this thesis are achieved, and the tasks are successfully completed:

1. Different EH methods are studied and evaluated in order to choose the appropriate method for generating electric power from wind flow and human motion. The applicable method for this research involves the use of a piezoelectric material.

2. Eight piezoelectric materials and different substrate materials are modelled and simulated to develop a piezoelectric cantilever beam consisting of two PZT-5J layers and a structural steel layer. The investigated piezoelectric cantilever beam has the lowest eigenfrequency 21.6 Hz and the best output power compared to the others.

3. Three different shapes are simulated to select the prototype that can ensure the highest output velocity of the wind flow. It is achieved by a cylinder with a narrow midsection, the output velocity of wind flow 5.2 m/s to 55.2 m/s when the input velocity between 1 and 20 m/s.

4. A power management and control unit are developed to decrease the electric loss and give stable electric output power. The control unit has been designed to be AC/DC converter and BQ25570 by Texas Instruments with lithium battery.

Based on the results, the electric output power under the external forces of wind flow and human motion acceleration between 2 and 87.8 mW

Further research could focus on finding a new source of energy and vibration or on discovering new methods of energy harvesting to make green energy available at any time and in any situation.

List of references

1. Goetzberger, A., Knobloch, J., & Voss, B. (1998). Crystalline silicon solar cells (p. 123). Chichester: Wiley.

2. Solar Panel (2013)[online] available at: https://www.pinterest.com/explore/pv-solar-panels/ [Accessed 10.11.2017]

3. Jie Chen (2015), Design and analysis of a thermoelectric energy harvesting system for powering sensing nodes in nuclear power plant.

4. Don Scansen (2011), Thermoelectric Energy Harvesting, [online] available at https://www.digikey.com/en/articles/techzone/2011/oct/thermoelectric-energy-harvesting [Accessed 01.01.2018]

5. Howells, C. A. (2009). Piezoelectric energy harvesting. Energy Conversion and Management, 50(7), 1847-1850.

6. Liu, Y. P., & Vasic, D. (2012). Self-powered electronics for piezoelectric energy harvesting devices. In Small-Scale Energy Harvesting. InTech.

7. Kang, M. G., Jung, W. S., Kang, C. Y., & Yoon, S. J. (2016). Recent progress on PZT based piezoelectric energy harvesting technologies. In Actuators (Vol. 5, No. 1, p. 5). Multidisciplinary Digital Publishing Institute.

8. Sirohi, J., & Mahadik, R. (2011). Piezoelectric wind energy harvester for low-power sensors. Journal of Intelligent Material Systems and Structures, 22(18), 2215-2228.

9. Mutsuda, H., Miyagi, J., Doi, Y., Tanaka, Y., Takao, H., & Sone, Y. (2014). Flexible piezoelectric sheet for wind energy harvesting. International Journal of Energy Engineering, 4(2), 67.

10. Matova, S. P., Elfrink, R., Vullers, R. J. M., & Van Schaijk, R. (2011). Harvesting energy from airflow with a michromachined piezoelectric harvester inside a Helmholtz resonator. Journal of Micromechanics and Microengineering, 21(10), 104001.

11. Sun, H., Zhu, D., White, N. M., & Beeby, S. P. (2013). A miniature airflow energy harvester from piezoelectric materials. In Journal of physics: Conference series (Vol. 476, No. 1, p. 012057). IOP Publishing.

12. Reitz, J. R., Milford, F. J., & Christy, R. W. (2008). Foundations of electromagnetic theory. Addison-Wesley Publishing Company.

13. El Rayes, K. A. R. E. M. (2013). Vibrations based energy harvesting. VLSI Egypt Magazine. Published on, 3.

14. Kwon, S. D., Park, J., & Law, K. (2013). Electromagnetic energy harvester with repulsively stacked multilayer magnets for low frequency vibrations. Smart materials and structures, 22(5), 055007.

15. Kim, S. H., Ji, C. H., Galle, P., Herrault, F., Wu, X., Lee, J. H., ... & Allen, M. G. (2009). An electromagnetic energy scavenger from direct airflow. Journal of Micromechanics and Microengineering, 19(9), 094010.

16. Ibrahim, M. (2014). Design, Modelling and Fabrication of a Hybrid Energy Harvester (Master's thesis, University of Waterloo).

17. Lesieutre, G. A., & Davis, C. L. (1997). Can a coupling coefficient of a piezoelectric device be higher than those of its active material?. Journal of intelligent material systems and structures, 8(10), 859-867.

18. Williams, C. B., & Yates, R. B. (1996). Analysis of a micro-electric generator for microsystems. sensors and actuators A: Physical, 52(1-3), 8-11.

19. Kim, S. G., Priya, S., & Kanno, I. (2012). Piezoelectric MEMS for energy harvesting. *MRS bulletin*, *37*(11), 1039-1050.

20. Roundy, S. J. (2003). Energy scavenging for wireless sensor nodes with a focus on vibration to electricity conversion (Doctoral dissertation, University of California, Berkeley).

21. Choi, Y. M., Lee, M. G., & Jeon, Y. (2017). Wearable Biomechanical Energy Harvesting Technologies. Energies, 10(10), 1483.

22. Versteeg, H. K., & Malalasekera, W. (2007). An introduction to computational fluid dynamics: the finite volume method. Pearson Education.

23. Lörcks, J. (1998). Properties and applications of compostable starch-based plastic material. Polymer degradation and stability, 59(1-3), 245-249.

24. Razak, I. S. A., Hashima, R. I. Z. R. Z., Nizam, S., & Soidb, M. (2012) A Design of Single Phase Bridge Full-wave Rectifier.

25. "Full wave rectifier", 2015.
[Online]. Available: http://www.ti.com/lit/ds/slusbh2e/slusbh2e.pdf. [Accessed 01.12.2017].

26. Guo, L., Hung, J. Y., & Nelms, R. M. (2002). PID controller modifications to improve steady-state performance of digital controllers for buck and boost converters. In Applied Power Electronics Conference and Exposition, 2002. APEC 2002. Seventeenth Annual IEEE (Vol. 1, pp. 381-388). IEEE.

27. Wu, T. F., Lai, Y. S., Hung, J. C., & Chen, Y. M. (2008). Boost converter with coupled inductors and buck–boost type of active clamp. IEEE Transactions on Industrial Electronics, 55(1), 154-162.

28. "bq25570 Nano Power Boost Charger and Buck Converter for Energy Harvester Powered Applications", (2015).
[Online]. Available: http://www.ti.com/lit/ds/slusbh2e/slusbh2e.pdf. [Accessed 01.02.2018].

29. Bagotsky, V. S., Skundin, A. M., & Volfkovich, Y. M. (2015). Electrochemical power sources: batteries, fuel cells, and supercapacitors. John Wiley & Sons.

30. Halper, M. S., & Ellenbogen, J. C. (2006). Supercapacitors: A brief overview. The MITRE Corporation, McLean, Virginia, USA, 1-34.

31. Brezesinski, T., Wang, J., Tolbert, S. H., & Dunn, B. (2010). Ordered mesoporous α-MoO 3 with iso-oriented nanocrystalline walls for thin-film pseudocapacitors. Nature materials, 9(2), 146.

32. Larcher, D., & Tarascon, J. M. (2015). Towards greener and more sustainable batteries for electrical energy storage. Nature chemistry, 7(1), 19.

33. "Standard Reduction Potentials (in Volts), 25oC", [Online]. Available: http://www.csudh.edu/oliver/chemdata/data-e.htm. [Accessed 12.12.2017].

34. Wang, Y., Liu, B., Li, Q., Cartmell, S., Ferrara, S., Deng, Z. D., & Xiao, J. (2015). Lithium and lithium ion batteries for applications in microelectronic devices: A review. Journal of Power Sources, 286, 330-345.

35. "Tadiran Lithium Ion Rechargeable Battery", (2013).
[Online]. Available: http://www.tadiranbat.com/assets/tli-1530a.pdf. [Accessed 09.04.2018].

Appendices

Appendix 1. Properties of different PZT material.

Appendix 2. Drawing of the first prototype.

Appendix 3. Drawing of the second prototype.

Appendix 4. Drawing of the third prototype.

Appendix 5. Datasheet of Lithium battery TLI

Appendix 6. Datasheet of BQ25570 by Texas Instrument

Properties of different PZT material

PROPERTY									
			PZT-8	**PZT-4**	**PZT-5H**	**PZT-5J**	**PZT-5A**	**PZT-4D**	**PZT-2**
Electromechanical coupling coefficient		K_p	0.51	0.54	0.65	0.64	0.63	0.62	0.45
		K_t	0.4	0.43	0.37	0.45	0.42	0.71	X
		K31	0.3	0.32	0.38	0.36	0.35	0.33	X
Frequency constant		N_p	2340	2290	1980	2030	2080	2010	X
	Hz ● m	N_t	2090	2080	1950	2050	2080	2180	X
		N31	1700	1690	1450	1460	1560	1560	X
Piezoelectric constant	$\times 10^{-12}$m/v	d_{33}	320	250	600	500	450	360	X
		d_{31}	-140	-100	-270	-210	-190	-145	X
Density	g/cm^3	r	7.6	7.8	7.8	7.7	7.8	7.7	7.6

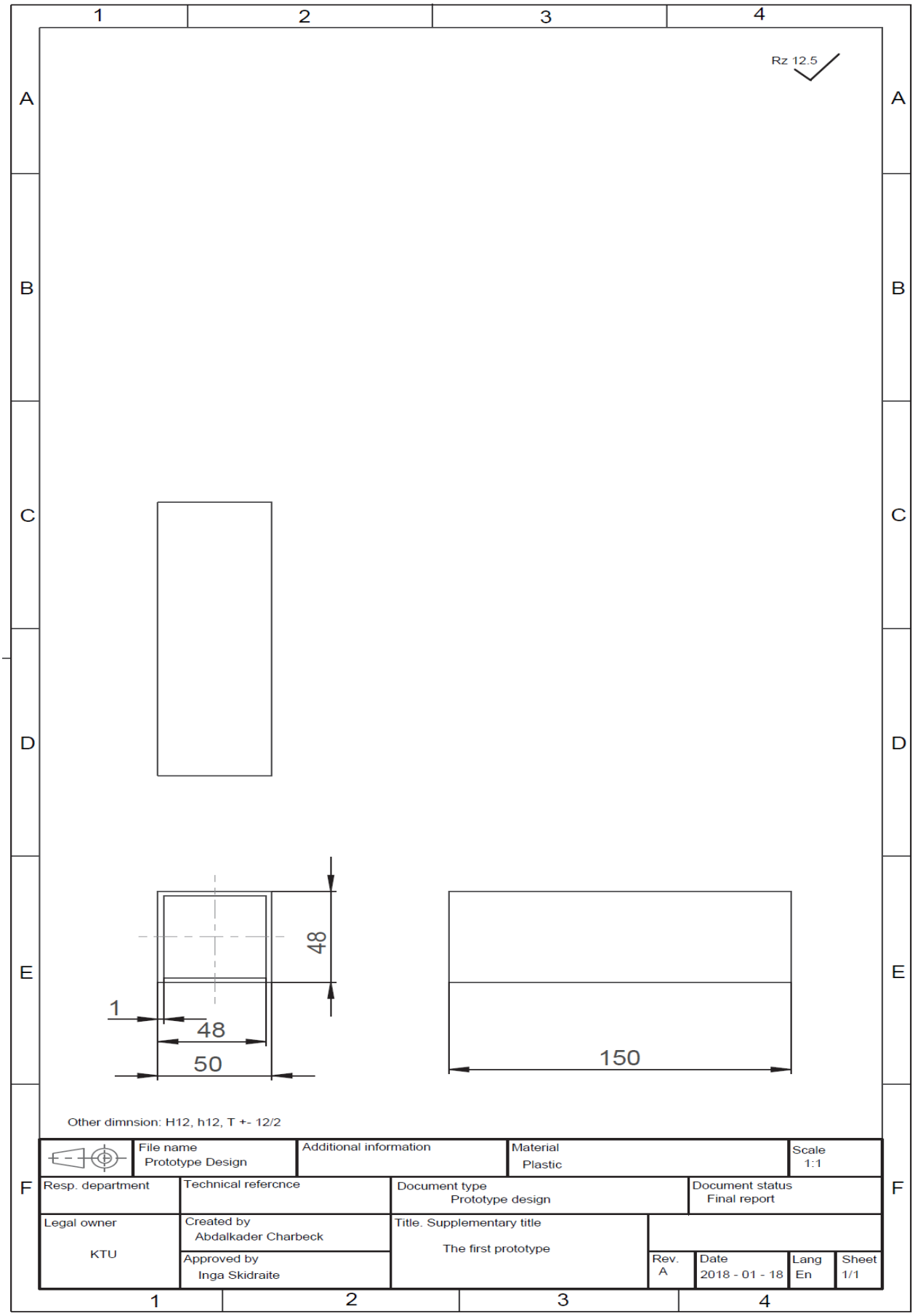
1
2
3
4
A
B
C
D
E
F
Rz 12.5
48
1
48
50
150
Other dimnsion: H12, h12, T +- 12/2
File name
Prototype Design
Additional information
Material
Plastic
Scale
1:1
Resp. department
Technical refercnce
Document type
Prototype design
Document status
Final report
Legal owner
KTU
Created by
Abdalkader Charbeck
Approved by
Inga Skidraite
Title. Supplementary title
The first prototype
Rev.
A
Date
2018 - 01 - 18
Lang
En
Sheet
1/1

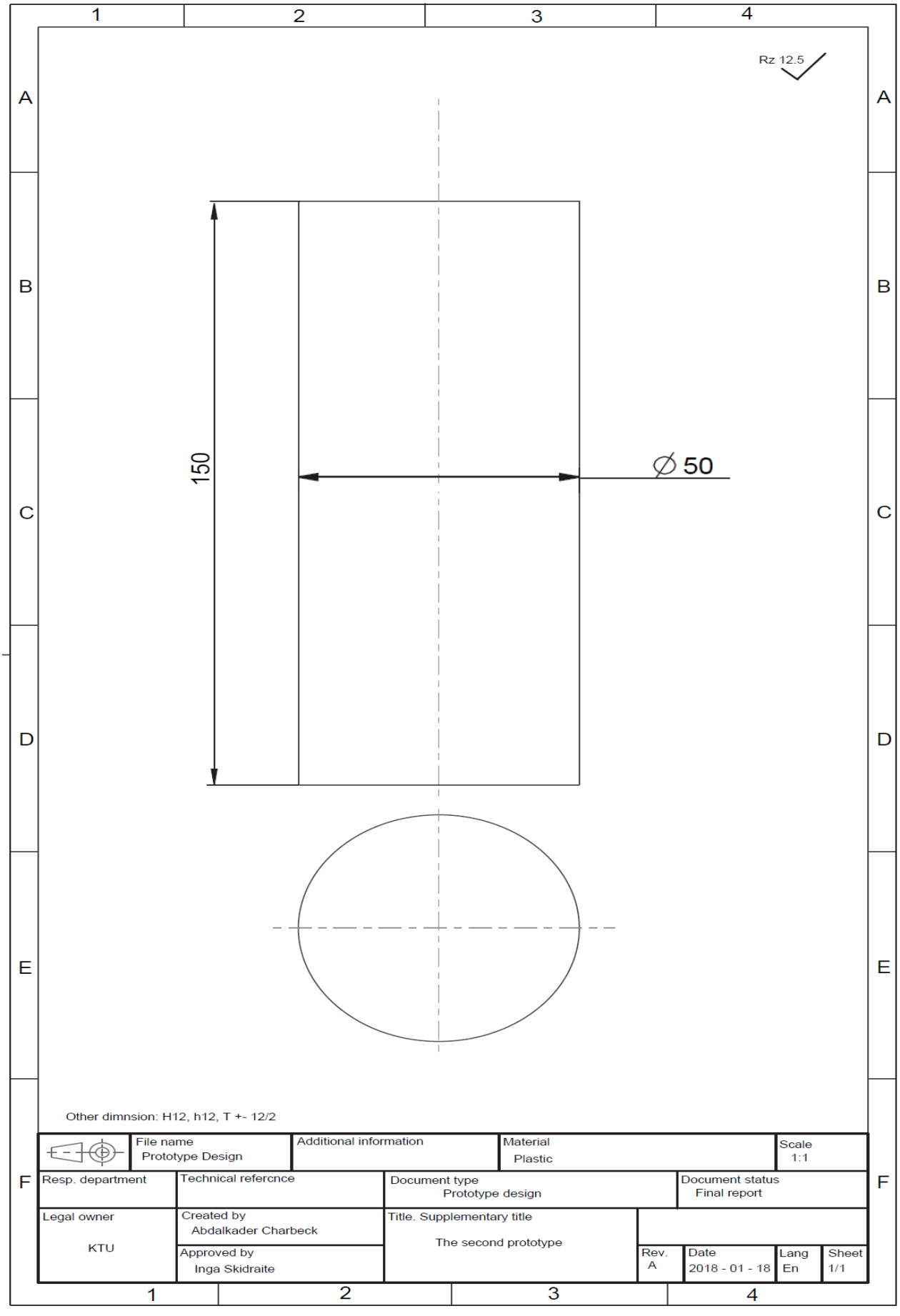
1
2
3
4
A
B
C
D
E
F
Rz 12.5
150
∅ 50
Other dimnsion: H12, h12, T +- 12/2
File name
Prototype Design
Additional information
Material
Plastic
Scale
1:1
Resp. department
Technical refercnce
Document type
Prototype design
Document status
Final report
Legal owner
KTU
Created by
Abdalkader Charbeck
Approved by
Inga Skidraite
Title. Supplementary title
The second prototype
Rev.
A
Date
2018 - 01 - 18
Lang
En
Sheet
1/1

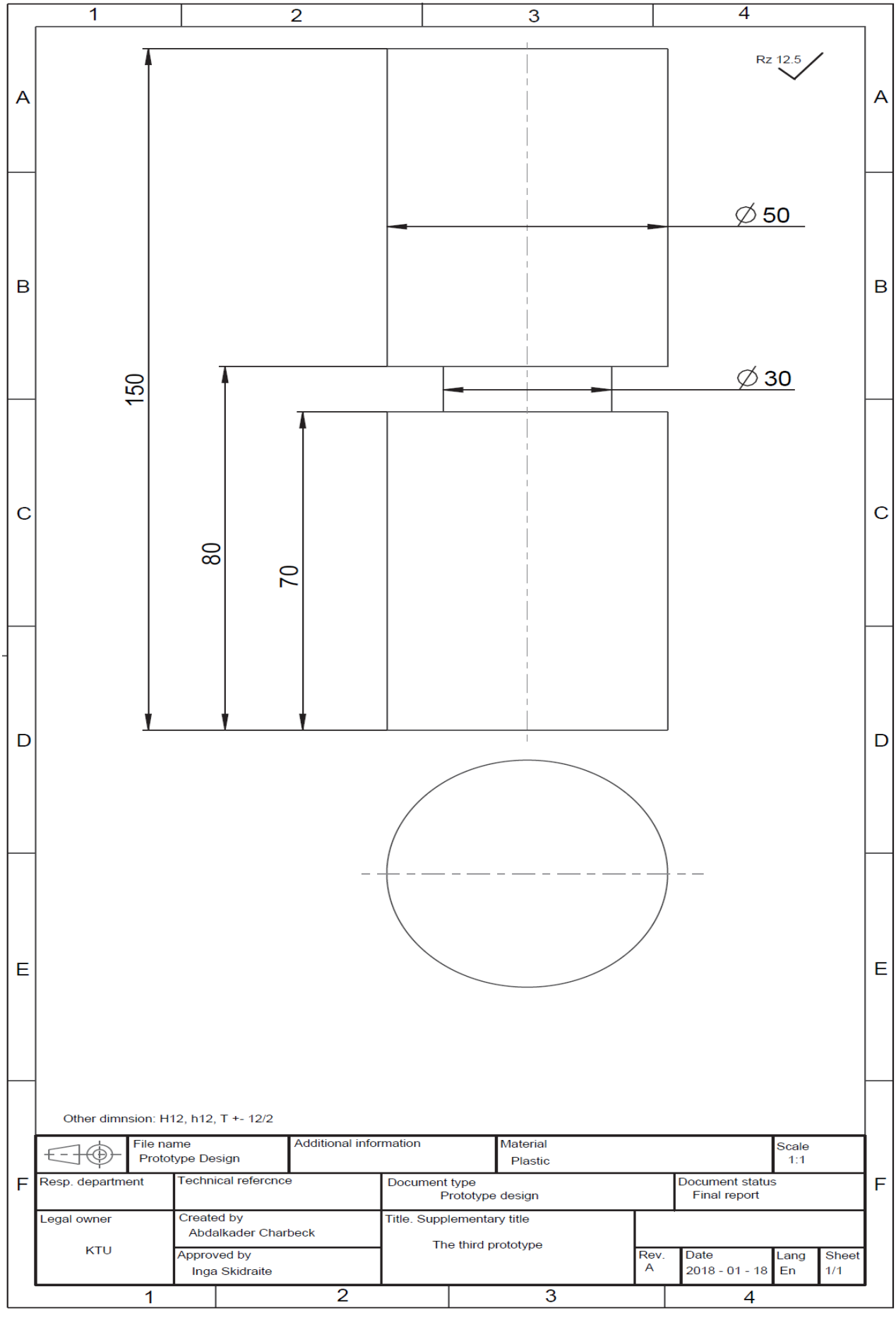
1
2
3
4
A
B
C
D
E
F
Rz 12.5
∅50
∅30
150
80
70
Other dimnsion: H12, h12, T +- 12/2
File name
Prototype Design
Additional information
Material
Plastic
Scale
1:1
Resp. department
Technical refercnce
Document type
Prototype design
Document status
Final report
Legal owner
KTU
Created by
Abdalkader Charbeck
Approved by
Inga Skidraite
Title. Supplementary title
The third prototype
Rev.
A
Date
2018 - 01 - 18
Lang
En
Sheet
1/1

Datasheet of Lithium battery TLI

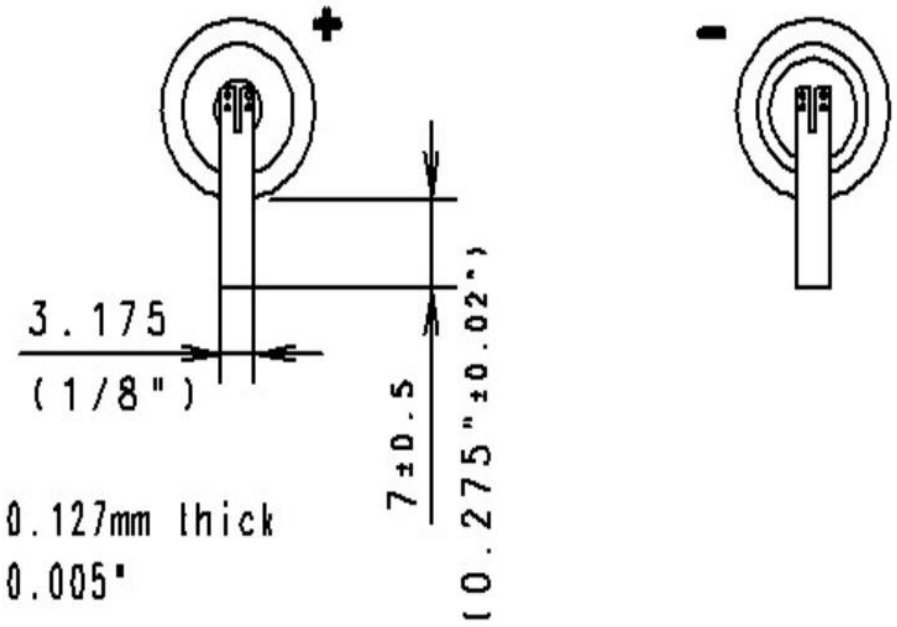

TADIRAN BATTERIES LTD

Tadiran Lithium Ion Rechargeable Battery
Model TLI-1530A

1. Scope

This specification applies to the 2/3AA size Lithium Ion Rechargeable battery supplied by Tadiran Batteries Ltd.

Notice: Charging circuit and application load profile have to be approved by Tadiran prior to the use of this cell.

2. Characteristics

2.1. Physical

2.1.1. Length: 27.4 mm Max.
2.1.2. Diameter: 15.1 mm Max
2.1.3. Weight: 9.9 gr. Max.

2.2. Electrical / Charge

2.2.1. Charge Voltage: 4.1 V
2.2.2. Charge Current: 50 mA Max.
2.2.3. Charge Method: CCCV (Constant Current/Constant Voltage)
2.2.4. End of Charge: 10 mA Max. per cell
2.2.5. Charge Temp. Range: -20 to +50 °C
Charge temperature can be extended to -40 ÷ +85 °C provided that the max. charge current is limited to 10 mA.

2.3. Electrical / Discharge

2.3.1. Nominal Current: 125 mA
2.3.2. End of Discharge: 2.5 V @ Room Temperature
2.3.3. Discharge Temp. Range: -40 to +85 °C
2.3.4. Performance Characteristics:

Item	Performance	Conditions
Battery Capacity	150 [mAh] 140 [mAh]	Discharge at 50 mA Discharge at 500 mA
Charge Discharge Cycles	140 [mAh]	After 100 cycles Discharge at 125 mA
Temperature	130 [mAh] 150 [mAh]	Discharge at -20 °C at 125 mA Discharge at 60 °C at 125 mA
Charge Retention (Reversible)	130 [mAh]	After 5 years at RT, Discharge at 125 mA
Impedance	Less than 175 mohm	Impedance at 1 KHz

Datasheet of BQ25570 by Texas Instrument

bq25570 Nano Power Boost Charger and Buck Converter for Energy Harvester Powered Applications

1 Features

- Ultra Low Power DC-DC Boost Charger
  - Cold-start Voltage: VIN ≥ 330 mV
  - Continuous Energy Harvesting From VIN as low as 100 mV
  - Input Voltage Regulation Prevents Collapsing High Impedance Input Sources
  - Full Operating Quiescent Current of 488 nA (typical)
  - Ship Mode with < 5 nA From Battery
- Energy Storage
  - Energy can be Stored to Re-chargeable Li-ion Batteries, Thin-film Batteries, Super-capacitors, or Conventional Capacitors
- Battery Charging and Protection
  - Internally Set Undervoltage Level
  - User Programmable Overvoltage Levels
- Battery Good Output Flag
  - Programmable Threshold and Hysteresis
  - Warn Attached Microcontrollers of Pending Loss of Power
  - Can be Used to Enable or Disable System Loads
- Programmable Step Down Regulated Output (Buck)
  - High Efficiency up to 93%
  - Supports Peak Output Current up to 110 mA (typical)
- Programmable Maximum Power Point Tracking (MPPT)
  - Provides Optimal Energy Extraction From a Variety of Energy Harvesters including Solar Panels, Thermal and Piezo Electric Generators

2 Applications

- Energy Harvesting
- Solar Chargers
- Thermal Electric Generator (TEG) Harvesting
- Wireless Sensor Networks (WSN)
- Low Power Wireless Monitoring
- Environmental Monitoring
- Bridge and Structural Health Monitoring (SHM)
- Smart Building Controls
- Portable and Wearable Health Devices
- Entertainment System Remote Controls

3 Description

The bq25570 device is specifically designed to efficiently extract microwatts (μW) to milliwatts (mW) of power generated from a variety of high output impedance DC sources like photovoltaic (solar) or thermal electric generators (TEG) without collapsing those sources. The battery management features ensure that a rechargeable battery is not overcharged by this extracted power, with voltage boosted, or depleted beyond safe limits by a system load. In addition to the highly efficient boosting charger, the bq25570 integrates a highly efficient, nano- power buck converter for providing a second power rail to systems such as wireless sensor networks (WSN) which have stringent power and operational demands. All the capabilities of bq25570 are packed into a small foot-print 20-lead 3.5-mm x 3.5-mm QFN package (RGR).

Device Information(1)

PART NUMBER	PACKAGE	BODY SIZE (NOM)
bq25570	VQFN (20)	3.50 mm × 3.50 mm

(1) For all available packages, see the orderable addendum at the end of the datasheet.

Typical Application Schematic

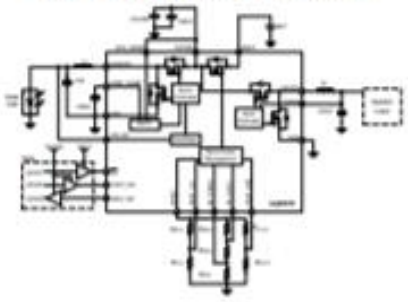

Charger Efficiency vs Input Voltage